Response to Anonymous Referee #1

General Comments: In this paper, Choi et al. analyzed black carbon (BC) and CO measurements at four remote/background sites in East Asia. They compared the measured BC/CO ratio with that from emission inventories, particularly the REAS inventory. They found that as compared with the measurements, BC/CO ratio in REAS is too high for Korea and too low for North Korea, probably due to certain emission factors in the transportation sector. They also conducted trajectory analyses to identify areas where emission estimates in REAS have large differences from measurements. Overall, this is an interesting study that provides some insights into the uncertainties of bottom-up emission inventories for East Asia. The topic should be of interest to the atmospheric chemistry and aerosol research community. The paper is generally well organized. Writing will need some improvements but is mostly understandable. There are, however, a few major concerns that should be addressed before the paper can be accepted for publication in Atmos. Chem. Phys.

Response: We thank the reviewer for carefully reviewing the manuscript and providing valuable comments. The following are our responses to your specific comments. For convenience, your comments are italicized and numbered. The line (L) numbers in the responses correspond to those in the revised manuscript. The changes in the revised manuscript are underlined in the responses as necessary, and are indicated as 'tracked changes' in the manuscript.

Specific comments:

1. *The authors claim harmonized BC/CO measurements but provide no evidence that the BC data are cross-validated between different sites. Have the authors conducted any side-by-side comparisons of the instruments involved? Can the authors provide an uncertainty estimate on the BC and CO measurements?*

   Unfortunately, we did not conduct a side by side comparison, except for between the sunset EC/OC analyzer and CLAP at Gosan (L170-L174), but there are many efforts to harmonize BC concentrations from MAAP with other instruments. Systematic harmonization among BC-measuring instruments, namely, COSMOS, MAAP, SP2, and EC/OC analyzer in Asia in locations both urban and remote is being developed (e.g., Kondo et al., 2011; Kanaya et al., 2013, 2016; Miyakawa et al., 2016, 2017; Taketani et al., 2016; Ohata et al., 2019). We added a more detailed description and references as follows:

   "… reported to have good agreement between instruments, including OC-EC analyzers (Sunset Laboratory Inc., USA) with optical corrections, single-particle soot photometers (SP2), continuous soot-monitoring systems (COSMOS) and multi-angle absorption photometers (MAAP 5012 Thermo Scientific) (e.g., Kondo et al., 2011; Kanaya et al., 2008, 2013, 2016; Miyakawa et al., 2016, 2017; Taketani et al., 2016; Ohata et al., 2019)." (L132-136)

   "It should be noted that we used a different mass absorption efficiency (MAE) value of 10.3 m^2 g^{-1}, as suggested by Kanaya et al. (2013), instead of the default MAE of 6.6 m^2

g^{-1}, ~~which showed perfect correlation with the COSMOS BC concentration (Kanaya et al., 2013)~~. <u>This value was validated with COSMOS, which showed a reliable performance with SP2 and OC-EC analyzer (Miyakawa et al., 2017; Kondo et al., 2011; Ohata et al., 2019) on a long-term basis at Fukue (Kanaya et al., 2016) and in Tokyo (Kanaya et al., 2013). The consistency between MAAP and SP2 at Noto was reported at ~10% (Taketani et al., 2016). At Fukuoka, a similar behavior was expected as the BC there would be a mixture from the continent and urban sources, as experienced at Fukue and Tokyo.</u>" (L150-158)

The uncertainties of the sunset EC/OC (L144) and MAAP (L160) were already mentioned, so we added the uncertainties of the BC and CO measurements as follows:

"The overall uncertainties of the BC and CO measurements were estimated to be less than 15% (except for Gosan, at 20%) and 5%, respectively. The overall regional ΔBC/ΔCO ratio varied from -0.7 (-8%) to 0.8 (10%) due to uncertainty." (L177-180)

Kondo, Y., Sahu, L., Moteki, N., Khan, F., Takegawa, N., Liu, X., Koike, M., and Miyakawa, T.: Consistency and Traceability of Black Carbon Measurements Made by Laser-Induced Incandescence, Thermal-Optical Transmittance, and Filter-Based Photo-Absorption Techniques, Aerosol Sci. Tech., 45, 295-312, 10.1080/02786826.2010.533215, 2011.

Miyakawa, T., Kanaya, Y., Komazaki, Y., Taketani, F., Pan, X., Irwin, M., and Symonds, J.: Intercomparison between a single particle soot photometer and evolved gas analysis in an industrial area in Japan: Implications for the consistency of soot aerosol mass concentration measurements, Atmos. Environ., 127, 14-21, https://doi.org/10.1016/j.atmosenv.2015.12.018, 2016.

Ohata, S., Kondo, Y., Moteki, N., Mori, T., Yoshida, A., Sinha, P. R., and Koike, M.: Accuracy of black carbon measurements by a filter-based absorption photometer with a heated inlet, Aerosol Sci. Tech., 53, 1079-1091, 10.1080/02786826.2019.1627283, 2019.

Taketani, F., Kanaya, Y., Nakayama, T., Ueda, S., Matsumi, Y., Sadanaga, Y., Iwamoto, Y., and Matsuki, A.: Property of Black Carbon Particles Measured by a Laser-Induced Incandescence Technique in the spring at Noto Peninsula, Japan, J. Aerosol Res., 31, 194-202, 10.11203/jar.31.194, 2016 (Abstract in English).

2. *The authors used the 14-day moving 5th percentile to determine baseline CO. I wonder if the authors can elaborate more on why this criterion is selected. In particular, from Figure 2b, one can see some fairly sudden, large changes in the baseline from time to time. One would expect the baseline CO to be mainly affected by (small) sources and chemistry over large background areas and the changes should be gradual.*

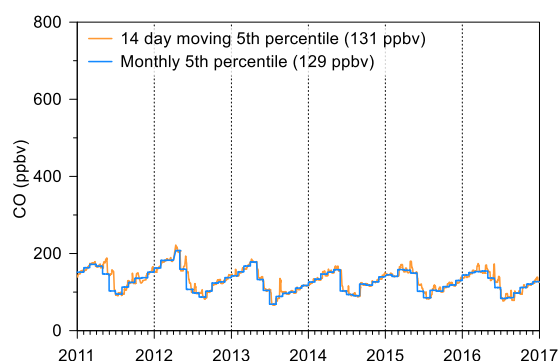We added a more detailed description of the CO baseline and its effects as follows:

"ΔCO was calculated by subtracting the baseline level ~~(determined as a 14-day moving 5th percentile)~~ from the observed CO mixing ratio. <u>Though there are several methods for estimating the CO baseline level (e.g., Matsui et al., 2011; Miyakawa et al. 2017; Oshima</u>

et al., 2012; Verma et al. 2011), the CO baseline in this study was regarded as a 14-day moving 5th percentile based on Kanaya et al. (2016)." (L199-203)

"The uncertainty of the BC/CO ratio that may arise from estimating the CO baseline by different methods and from allocation methods involving selecting different altitudes are discussed in the Supplement (S4)." (L227-229)

In the supplement (S4), we added a paragraph and figure as follows:

"First, there are several ways to determine the CO baseline, mainly depending on the measurement period. For intensive measurement periods, the CO baseline can be calculated from the 5th percentile of data (Matsui et al. 2011; Miyakawa et al., 2017) or the x-intercept of the best-fit line between BC and CO (Oshima et al., 2012). It can also be calculated by the 5th percentile of the CO concentration from monthly (Verma et al. 2011) or moving 14-day (Kanaya et al. 2016) from long-term measurements. We tested the difference in CO baselines calculated from the 5th percentile of the moving 14-day (our method) and monthly CO data (Figure S5).

Figure S5. Time series of CO baselines calculated by different methods (14-day moving 5th and monthly 5th percentiles) at Noto.

The difference in the CO baseline from the monthly data was slightly lower (-2 ppbv; -1.9%) than our estimation. Moreover, the mean $\Delta BC/\Delta CO$ ratios from the two different methods did not show significant differences (5.82 ng m^{-3} ppb^{-1} for our estimation and 5.87 ng m^{-3} ppb^{-1} for monthly data), when Welch's t-test was applied ($p > 0.1$)."

Basically, the fluctuation of the CO baseline over a large scale could be regarded as seasonal variation, increasing from October to April and then decreasing until September. Rapid peak concentrations with finer scales were also considered as effects of air pollution events, but these sudden changes could be negligible when compared to the monthly 5th percentile baseline, which showed more smooth variation.


3. *The authors compared measured BC/CO ratio with different emission inventories, but the focus is on REAS. Have there been any recent updates to REAS in recent years? It looks like 2008 is the last year for which REAS provides emission estimates. Given that measurements were mostly made in the 2010s and that East Asia has been undergoing fast changes in terms of emissions, would it be more useful to focus, instead, on emission inventories that have more recent estimates (such as EDGAR and MIX Asia)?*

Unfortunately, the new version of REAS emission inventory (V3) is under development, so we could not compare the BC and CO emissions after 2008 in REAS inventory. Though the BC and CO emission rates over East Asia have dramatically changed since 2000s, there were no significant changes in the BC/CO ratio since 2008 when we checked it using the

EDGAR and MIX emission inventories. We added relevant sentences as follows:

"It should be noted that there were no significant changes in trends for the long-term variation of the ΔBC/ΔCO ratios of all sites, as well as BC/CO ratios from the Emissions Database for Global Atmospheric Research (EDGAR version 4.3.2; Crippa et al. 2018) emission inventory since 2008 and the MIX emission inventory (Li et al., 2017) in 2008 and 2010 (Figure S6). This result implied that comparison between the measurements and the REAS emission inventory was a reasonable approach, even though the time scale between them did not match." (L278-284)

We also discussed the EDGAR and MIX emission inventories in detail. (L416-424 and L471-483)
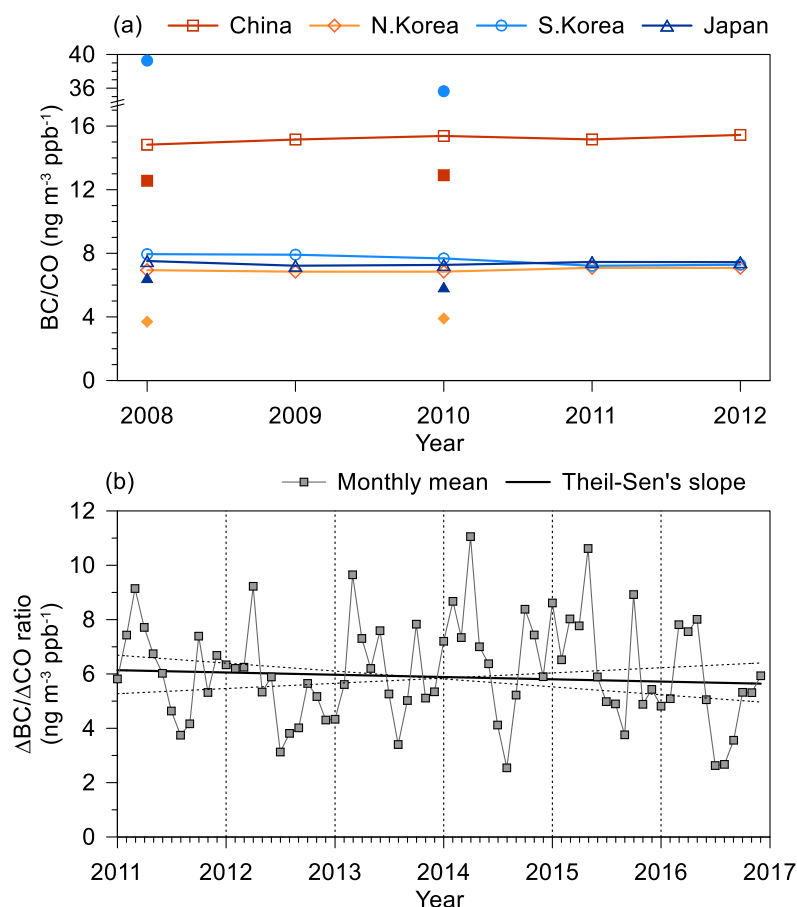
Figure S6. (a) Time series of the BC/CO ratios from the Emissions Database for Global Atmospheric Research (EDGAR v4.3.2; open symbols) during 2008 – 2012 and MIX emission inventory (filled symbols) in 2008 and 2010. (b) Time series of the monthly means of the ΔBC/ΔCO ratio with Theil-Sen's slope during the measurement periods at Noto. The Theil-Sen's slope of the ΔBC/ΔCO ratio indicated a slight decreasing trend of the ΔBC/ΔCO ratio at -0.08/year; but the trend was statistically insignificant ($p > 0.1$). Insignificant trends of the ΔBC/ΔCO ratio were also observed at the other sites.

Technical comments:

4

4. *Section 2.2, it is not clear whether there is a size cut for EC/OC or MAPP measurements? Table 2, from the table it appears that the baseline CO (difference between CO and deltaCO) is quite different between different sites, for example, between Gosan and Fukuoka. Can the authors comment on that?*

The size cut information for EC/OC and MAAP was already mentioned in Section 2.2 as follows:

EC/OC analyzer: "Hourly elemental carbon (EC) concentrations in $PM_{2.5}$ at the Baengnyeong site…" (L137)

MAAP: "At both the Noto and Fukuoka sites, $PM_{2.5}$ BC concentrations were measured using a MAAP." (L145)

However, we mentioned the size cut information again in Table 1 for clarity.

We also added data for CO baseline in Table 2 and a brief comment on the differences in the CO baseline, as follows:

"Despite the suburban location of Fukuoka, the BC ~~and ΔCO concentrations were~~ concentration was even lower than ~~those~~that of Baengnyeong, However, the CO baseline concentration was highest among the measurement sites suggesting the influence of local sources, though it could be varied depending on geographical location. To check influence of local pollution at Fukuoka, we tested by applying more stringent CO baseline criteria (14-days moving 2 % percentile; ~166 ppbv). As a result, there was no significant changes in our results (less than -4 %).~~, indicating that the measurement site could not be seriously influenced by local sources.~~" (L238-245)

5. *Line 355-362: can the authors comment on what EDGAR may have done correctly to get a better overall comparison with measurements in terms of BC/CO ratio?*

We added a description of the EDGAR inventory as follows:

"As a result, the BC/CO ratio from EDGAR falls within a reasonable range as 6.85 ng m^{-3} ppb^{-1}, indicating agreement with the measured ratio (7.3 ng m^{-3} ppb^{-1}). This is because the ratio in EDGAR CO emission rates relative to REAS rates (30% of REAS) was much smaller than that for EDGAR BC (56% of REAS; Table 3), especially in the road transportation (9% for CO and 21% for BC) and industry sectors (38% for CO and 51% for BC)." (L402-407)

6. *Line 375: have the authors tested other thresholds for trajectory altitude? Does the selection of this threshold have any impacts on the results?*

Thank you for pointing out the possibility of discrepancies due to the different altitudes used as criteria. We added relevant information mentioning this effect as follows:

"The uncertainty of the BC/CO ratio that may arise from estimating the CO baseline by different methods and from allocation methods involving selecting different altitudes are discussed in the Supplement (S4)." (L227-229)

In supplement (S4), we added a paragraph and figure as follows:

"Second, we also checked the difference in ΔBC/ΔCO which can be caused by applying 1.5 km as a threshold to determine the dominant emission region. There was no significant difference in the regional ΔBC/ΔCO ratios between 2.5 and 1.5 km when Welch's t-test was applied ($p \geq 0.1$). For the seasonal variation, though five cases (spring, fall and winter in East China, fall in North China and winter in Northeast China) of recalculated REAS BC/CO values showed significant differences ($p < 0.05$), the ratios of those cases varied within ± 1.4 ng m^{-3} ppb^{-1} ($\pm 15\%$), indicating that the MFBs were preserved. From these results, we confirmed the representativeness of our regional and seasonal ΔBC/ΔCO analysis."
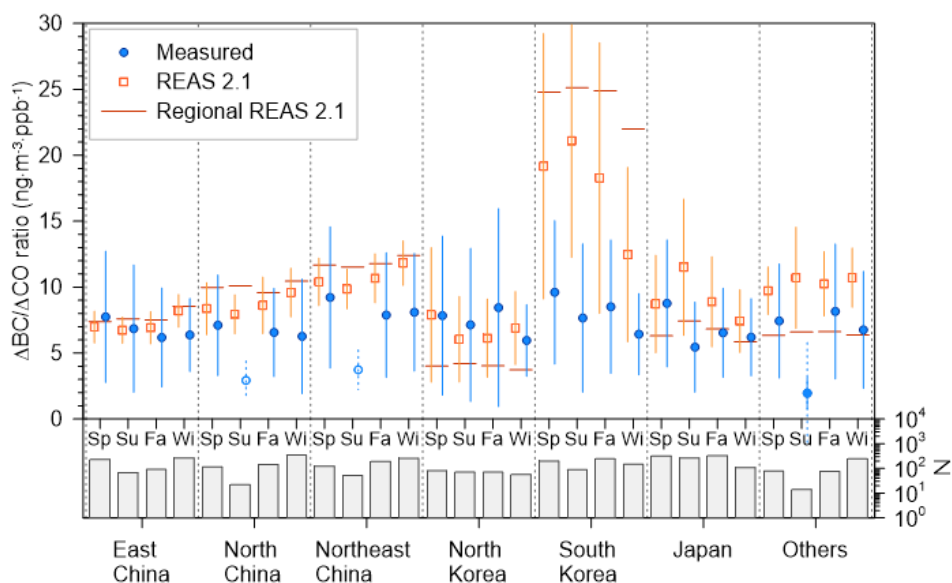
7. *Figure 3: is the REAS mean (horizontal lines) weighted based on total emissions from each grid cell within the domain?*

Yes. The horizontal lines for REAS were the total average of the ΔBC/ΔCO ratio of each dominant emission region, regardless of passing the trajectory. We added the detailed description to the caption of Figure 3 as follows:

"… The solid red horizontal lines depict the overall mean BC/CO ratios of dominant emission regions from the REAS version 2.1 emission inventory (Kurokawa et al., 2013)."

8. *Figure 4: some of the seasons have few data points and the comparison may not be valid for those sites and seasons. Also please describe in the caption how the values for the squares are calculated.*

In Figure 4, we revised the data, adding a few points as open circles, and added an explanation of the open squares in the caption as follows:

Figure 4. The seasonal ΔBC/ΔCO ratios from four measurement sites (filled blue circles) and recalculated REAS BC/CO ratios <u>according to the pathway of the trajectory (open orange</u>

squares), depending on the dominant emission region. The symbols with vertical lines are the means and standard deviations of the ΔBC/ΔCO ratios. Open-circle symbols with dashed vertical lines indicate data excluded because of a low number of data (≤ 50). The horizontal lines for each region indicate the overall mean values of the ΔBC/ΔCO ratios of dominant emission regions from the REAS version 2.1 emission inventory (Kurokawa et al., 2013). The bar graph on the bottom indicates the number of data in each season and the dominant emission region. The symbols with vertical lines are the means and standard deviations of the ΔBC/ΔCO ratios. The abbreviation of 'Sp' to 'Wi' indicates spring to winter.

Regional variability in black carbon and carbon monoxide ratio from long-term observations over East Asia: Assessment of representativeness for BC and CO emission inventories

Yongjoo Choi[1*], Yugo Kanaya[1], Seung-Myung Park[2], Atsushi Matsuki[3], Yasuhiro Sadanaga[4], Sang-Woo Kim[5], Itsushi Uno[6], Xiaole Pan[7], Meehye Lee[8], Hyunjae Kim[2], Dong Hee Jung[2]

[1] Research Institute for Global Change, Japan Agency for Marine-Earth Science and Technology (JAMSTEC), Yokohama, 2360001, Japan

[2] Division of Climate & Air Quality Research, National Institute of Environmental Research, Kyungseo-dong, Seo-Gu, Incheon 404170, Korea

[3] Institute of Nature and Environmental Technology, Kanazawa University, Kanazawa 9201192, Japan

[4] Department of Applied Chemistry, Graduate School of Engineering, Osaka Prefecture University, 1-1 Gakuen-cho, Naka-ku, Sakai, Osaka 5998531, Japan

[5] School of Earth and Environmental Sciences, Seoul National University, Seoul, Korea

[6] Research Institute for Applied Mechanics, Kyushu University, Kasuga Park 6-1, Fukuoka, 816-8580, Japan

[7] Institute of Atmospheric Physics, Chinese Academy of Sciences, Beijing, China

[8] Department of Earth and Environmental Sciences, Korea University, Seoul, Korea

*Correspondence to: Yongjoo Choi (choingjoo@jamstec.go.jp)

Abstract

The black carbon (BC) and carbon monoxide (CO) emission ratios were estimated and compiled from long-term, harmonized observations of the ΔBC/ΔCO ratios under conditions unaffected by wet deposition at four sites in East Asia, including two sites in Korea (Baengnyeong and Gosan) and two sites in Japan (Noto and Fukuoka). Extended spatio-temporal coverage enabled estimation of the full seasonality and elucidation of the emission ratio in North Korea for the first time. The estimated ratios were used to validate the Regional Emission inventory in ASia (REAS) version 2.1 based on six study domains (East China, North China, Northeast China, South Korea, North Korea, and Japan). We found that the ΔBC/ΔCO ratios from four sites converged into a narrow range (6.2 – 7.9 ng m^{-3} ppb^{-1}), suggesting consistency in the results from independent observations and similarity in source profiles over the regions. The BC/CO ratios from the REAS emission inventory (7.7 ng m^{-3} ppb^{-1} for East China – 23.2 ng m^{-3} ppb^{-1} for South Korea) were overestimated by factors of 1.1 for East China to 3.0 for South Korea, whereas the ratio for North Korea (3.7 ng m^{-3} ppb^{-1} from REAS) was underestimated by a factor of 2.0, most likely due to inaccurate emissions from the road transportation sector. Seasonal variation in the BC/CO ratio from REAS was found to be the highest in winter (China and North Korea) or summer (South Korea and Japan), whereas the measured ΔBC/ΔCO ratio was the highest in spring in all source regions, indicating the need for further characterization of the seasonality when creating a bottom-up emission inventory. At levels of administrative districts, overestimation in Seoul, the southwestern regions of South Korea, and Northeast China was noticeable, and underestimation was mainly observed in the western regions in North Korea, including Pyongyang. These diagnoses are useful for identifying regions where revisions in the inventory are necessary, providing guidance for the refinement of BC and CO emission rate estimates over East Asia.

1 Introduction

Black carbon (BC), emitted from the incomplete combustion of fossil fuel and/or biomass burning, absorbs solar radiation and reduces the surface albedo of snow/ice after dry/wet deposition (Samset, 2018; Bond et al., 2013); thereby augmenting the global warming trend primarily induced by increased levels of carbon dioxide (CO_2) (Ramanathan and Carmichael, 2008; Jacobson, 2001; Myhre et al., 2013). In addition to global warming effects, BC is significantly associated with cardiovascular mortality (Smith et al., 2009; Geng et al., 2013), and is more related to health effects than $PM_{2.5}$ (particulate matter having an aerodynamic diameter ≤ 2.5 μm) (Janssen et al., 2011, 2012; Loomis et al., 2013).

In particular, the BC emissions from China, which accounted for 31% of the total annual global emissions in 2012 (Crippa et al., 2018), showed an increasing trend from 1970 to 2012 (Kurokawa et al., 2013; Ohara et al., 2007; Crippa et al., 2018). To enhance the understanding of the behavior of BC in the atmosphere, it is essential to obtain a reliable BC concentration along with model simulations based on accurate bottom-up emission inventories. The bottom-up emission inventories may be subject to large uncertainties associated with emission factors from various types of combustion sources, countries and species (Kurokawa et al., 2013), although the uncertainty in BC emissions decreased from 160.2% in 1970 to 74.3% in 2012 (Crippa et al., 2018). BC and carbon monoxide (CO) are byproducts of the incomplete combustion of carbon-based fuels, and the ratio between ΔBC (the difference from the baseline level) and ΔCO could be a useful parameter for characterizing combustion types. Using these characteristics, past studies used the ΔBC/ΔCO ratio to identify emission source types (Guo et al., 2017; Pan et al., 2011; 2013; Zhu et al., 2019) and/or validate BC emissions from bottom-up inventories (Han et al., 2009; Wang et al., 2011; Verma et al., 2011; Sahu et al., 2009; Kondo et al., 2006). However, it was hard to diagnose the accuracy of emission inventories over East Asia from those studies because either data covering short, intensive measurement periods at a single site were used or the studied source regions did not necessarily match the administrative districts for which a detailed emission inventory was constructed. In addition, BC concentrations can differ depending on the instruments and operation protocols used for observations—such discordance yet poses a major obstacle to obtaining a comprehensive understanding. Kondo (2015) compiled ΔBC/ΔCO ratios from systematic observations in Asia. However, information during the 2010s, when emissions patterns changed significantly, has

83 not been covered. Kanaya et al. (2016) used observations at Fukue Island for 6 years (2009-
84 2015) to derive a region-specific ΔBC/ΔCO emission ratio. However, the seasons were limited
85 to autumn-spring, and the footprint over each source region was still limited, as observations
86 at a single site were analyzed.

87   In this study, we investigated the ΔBC/ΔCO ratios from long-term measurements at four
88 measurement sites (two Korean and two Japanese sites which were measured for more than a
89 year) over East Asia in order to comprehensively evaluate the Regional Emission inventory in
90 ASia (REAS) version 2.1 based on the 2008 emission inventory (Kurokawa et al., 2013) of BC
91 and CO with sufficient spatio-temporal coverage. The REAS inventory comprises emissions
92 data from 30 Asian countries and regions, including China, North Korea, South Korea and
93 Japan, between the years 2000 and 2008 at a 0.25°×0.25° horizontal resolution. The emissions
94 sources consisted of power plants, combustible and non-combustible sources in industry, on-
95 road and off-road sources in transport, and residential and other activities, such as agricultural
96 activities and evaporative sources (Han et al., 2015; Itahashi et al., 2017; Kurokawa et al., 2013;
97 Saikawa et al., 2017; Uno et al., 2017). The improved spatio-temporal coverage enabled
98 estimation of the full seasonality and elucidation of the emissions ratio from North Korea for
99 the first time. By comparing the regional and seasonal ΔBC/ΔCO ratios between the REAS
100 emission inventory and the measurements, this study identifies the points of improvement for
101 bottom-up emission inventories.

102

103 **2 Methodology**

104 **2.1 Measurement sites and periods**

105 Figure 1 shows the locations of the measurement sites in this study. Both Baengnyeong
106 (124.63 °E, 37.97 °N) and Gosan (126.17°E, 33.28 °N) are representative background sites in
107 Korea. The Baengnyeong site is an intensive measurement station operated by the Korean
108 Ministry of Environment. The Gosan site is a supersite of many international campaigns, such
109 as Aerosol Characterization Experiments (ACE)-Asia (Huebert et al., 2003), Atmospheric
110 Brown Cloud (ABC) (Nakajima et al., 2007) and Cheju ABC Plume–Monsoon Experiment
111 (CAPMEX) (Ramana et al., 2010). Since the two sites in Korea are located in the western
112 region of the Korean peninsula with similar longitudes but different latitudes, these sites are

113 suitable for monitoring pollutant transport from China, North Korea (especially Baengnyeong)

114 and South Korea. In Japan, the Fukuoka site (33.52 °N, 130.47 °E) is located at the Chikushi

115 Campus of Kyushu University located in the suburbs of Fukuoka, and the site is the largest

116 center of commerce on the island of Kyushu (Itahashi et al., 2017; Uno et al., 2017). The Noto

117 site (37.45 °N, 137.36 °E) is located at the Ground-based Research Observatory (NOTOGRO),

118 which has been apart from Kanazawa and Toyama, the nearest provincial cities, by

119 approximately 115 km southwest and 85 km south, respectively. Therefore, Noto is a suitable

120 place for monitoring the background concentrations and/or outflows of pollution from the

121 Asian continent (Ueda et al., 2016). The measurement periods were commonly in the early

122 2010s, while slight differences were present among the sites (Table 1). The longest

123 measurement period was in Noto for approximately six years (from 2011 to 2016), followed

124 by those in Baengnyeong (five years), Gosan (three years), and Fukuoka (one and a half years).

125 The measurements in Baengnyeong did not include 2011 to 2012 due to the absence of CO

126 data.

127

2.2 Instruments

129 It is crucial to ensure reliable atmospheric BC concentrations, which were measured by

130 different instruments, by excluding the effects of co-existing scattering particles. To keep the

131 harmonization, we considered BC concentrations to be reliable when the data were measured

132 by pre-validated instruments reported to have good agreement between instruments, including

133 OC-EC analyzers (Sunset Laboratory Inc., USA) with optical corrections, single-particle soot

134 photometers (SP2), continuous soot-monitoring systems (COSMOS) and multi-angle

135 absorption photometers (MAAP 5012 Thermo Scientific) (e.g., Kondo et al., 2011; Kanaya et

136 al., 2008, 2013, 2016; Miyakawa et al., 2016, 2017; Taketani et al., 2016; Ohata et al., 2019).

137 Hourly elemental carbon (EC) concentrations in $PM_{2.5}$ at the Baengnyeong site were

138 measured by a model-4 semi-continuous OC-EC field analyzer using the thermal/optical

139 transmittance (TOT) method and the non-dispersive infrared (NDIR) method based on NIOSH

140 method 5040 (NIOSH, 1996). The particles passed through a $PM_{2.5}$ cyclone with 8.0 L/min and

141 a carbon impregnated multi-channel parallel plate diffusion denuder (Turpin et al., 2000), and

142 were collected on a quartz fiber filter during 45 min. OC and EC were then analyzed during

143 the last 15 min. The detection limit of EC, which is defined as twice the average of the field

144 blanks, was reported to be 30 ng m^{-3}, and the precision of EC was 7.5% (Park et al., 2013).

145   At both Noto and Fukuoka sites, PM$_{2.5}$ BC concentrations were measured using a MAAP.

146 The BC concentration is converted from the absorption coefficients, which were determined

147 by measuring both the transmittance and reflectance of a filter loaded with aerosols. Because

148 the MAAP installed a light detector that locates light reflected from the filter at 130° and 165°

149 from the illumination direction (Petzold et al., 2005), the MAAP can correct for scattering

150 particle effects. It should be noted that we used a different mass absorption efficiency (MAE)

151 value of 10.3 m^2 g^{-1}, as suggested by Kanaya et al. (2013), instead of the default MAE of 6.6

152 m^2 g^{-1}, ~~which showed perfect correlation with the COSMOS BC concentration (Kanaya et al.,~~

153 ~~2013).~~. This value was validated with COSMOS, which showed a reliable performance with

154 SP2 and OC-EC analyzer (Miyakawa et al., 2017; Kondo et al., 2011; Ohata et al., 2019) on a

155 long-term basis at Fukue (Kanaya et al., 2016) and in Tokyo (Kanaya et al., 2013). The

156 consistency between MAAP and SP2 at Noto was reported at ~10% (Taketani et al., 2016). At

157 Fukuoka, a similar behavior was expected as the BC there would be a mixture from the

158 continent and urban sources, as experienced at Fukue and Tokyo. The reported minimum

159 detection limit of the MAAP was different depending on the averaging time as 12 ng m^{-3} for

160 one hour and 64 ng m^{-3} for one minute by applying the revised MAE (10.3 m^2 g^{-1}).

161   The Gosan site has monitored BC concentrations using a continuous light absorption

162 photometer (CLAP) with three wavelengths including 467, 528, and 652 nm (Cho et al., 2019).

163 Through PM$_1$ and PM$_{10}$ impactors, which were switched every 30 min, the particles were

164 collected on 47-mm diameter glass-fiber filters (Pallflex type E70-2075W). The volumetric

165 flow rate was 1 L/min. The raw absorption coefficient of the CLAP was corrected using the

166 methods of Bond et al. (1999) to eliminate effects due to filter loading errors. The absorption

167 coefficient at 528 nm was used to determine the BC concentration by applying 10 m^2 g^{-1} for

168 MAE. In this study, we used the PM$_1$ BC concentration because BC particles mainly exist in

169 less than 1 μm (Miyakawa et al., 2017; Bond et al., 2013). Although the uncertainty derived

170 from scattering particles was reported to be ~25% at Gosan (Ogren et al., 2017), the BC from

171 CLAP was verified by comparison with a co-located semi-continuous OC-EC field analyzer

172 (Lim et al., 2012). The slope of the best fit line through the origin was close to one as 1.17,

173 implying that the PM$_1$ BC concentration from CLAP was well consistent with that from PM$_{2.5}$

174 EC.

175   Hourly CO concentrations were measured by a gas filter correlation CO analyzer (Model

176   300EU, Teledyne-API Inc.) at Baengnyeong and nondispersive infrared absorption

177   photometers (48C, Thermo Scientific) at the other three sites. The overall uncertainties of the

178   BC and CO measurements were estimated to be less than 15% (except for Gosan, at 20%) and

179   5%, respectively. The overall regional ΔBC/ΔCO ratio varied from -0.7 (-8%) to 0.8 (10%) due

180   to uncertainty.

181

2.3 ΔBC/ΔCO ratio and allocation of the dominant emission region

183   To identify the origin of BC and CO emission sources, backward trajectories at 500 m during

184   the past five days (120 hours) were calculated by the Hybrid Single Particle Lagrangian

185   Integrated Trajectory (HYSPLIT) 4 model (Draxler et al., 2018) for every six hour interval (00,

186   06, 12 and 18 UTC) using the Global Data Assimilation System (GDAS) with a horizontal

187   resolution of 1° × 1°, as the GDAS with 0.5° resolution did not account for vertical motion (Su

188   et al., 2015). The spatial distribution of the number of endpoints for backward trajectories from

189   the four measurement sites revealed the large spatial coverage of the footprint over East Asia

190   (Figure S1). These four sites could be representative for monitoring outflows from China and

191   Korea because of the dominance of wintertime monsoons. Moreover, the footprint of the Noto

192   site could cover the middle part of Japan, such as the Kanto, Chubu, and Kansai regions. To

193   exclude cases with wet deposition influence, the accumulated precipitation along with

194   trajectory (APT) was calculated over the past 72 hours (Kanaya et al., 2016; Oshima et al.,

195   2012), and we only used cases with APT = 0.

196   As aforementioned, BC and CO are commonly emitted from incomplete fuel combustion,

197   and the ΔBC/ΔCO ratio is used to evaluate the bottom-up emission inventory as a

198   representative indicator, preserving the emission ratio when wet removal is not influential

199   (Kanaya et al., 2016). ΔCO was calculated by subtracting the baseline level (determined as a

200   14-day moving 5th percentile) from the observed CO mixing ratio. Though there are several

201   methods for estimating the CO baseline level (e.g., Matsui et al., 2011; Miyakawa et al. 2017;

202   Oshima et al., 2012; Verma et al. 2011), the CO baseline in this study was regarded as a 14-day

203   moving 5th percentile based on Kanaya et al. (2016). On the other hand, ΔBC is the BC

204   concentration as is (BC baseline = 0), because the baseline concentrationatmospheric lifetime

14

of BC ~~was assumed~~is estimated to be ~~zero.~~several days (Park et al., 2005), in contrast to that of CO, which has a one- or two-month lifetime (Bey et al. 2001). It should be noted that we used the CO concentration when it was higher than the moving 25th percentile of CO, so that only data with meaningful enhancement was employed.

To determine the dominant emission region of each sample, we calculated the residence time over the six regions (East China, North China, Northeast China, North Korea, South Korea, and Japan) using backward trajectories covering the previous 72 hours. Hourly endpoints with altitudes of less than 2.5 km were counted (Kanaya et al., 2016). Based on the fractions of the total 73 hours, the highest fraction of the region was classified as the dominant emission region when the fraction of the frequency was higher than 5% to secure statistics (S1; Figure S2). In addition, we checked (1) the dry deposition effect during the traveling time ~~and~~, (2) the influences of other regions on $\Delta BC/\Delta CO$ depending on the residence time~~.~~ and (3) biomass burning events that could cause distortion producing higher $\Delta BC/\Delta CO$ values. As a result, it was determined that there was no significant dry deposition effect (S2; Figure S3) or interrupted by other regions (S3; Figure S4), implying that the BC/CO ratio was preserved regardless of the residence time over other regions when the threshold ($N > 5$) of each bin (20% interval) was satisfied. In addition, the influences from biomass burning were minimized during long-term periods, as confirmed by no significant difference between the ratios produced by including and excluding biomass burning events selected by the Moderate Resolution Imaging Spectroradiometer (MODIS) Fire Information for Resource Management System (FIRMS). Miyakawa et al. (2019) also pointed out that ~90% of BC in springtime at Fukue originated from the combustion of fossil fuel.

The uncertainty of the BC/CO ratio that may arise from estimating the CO baseline by different methods and from allocation methods involving selecting different altitudes are discussed in the Supplement (S4).

3 Results and discussion

3.1 Seasonal variation in BC and CO

The BC, CO, and ΔCO concentrations are summarized in Table 2. The mean BC and ΔCO concentrations were highest in Baengnyeong, followed by Fukuoka, Gosan, and Noto,

according to the distance from the main BC and CO emission sources, China. Although the levels at Baengnyeong and Gosan were high, they maintained regional representativeness, as the BC concentration levels were lower than those at urban sites such as Daejon ($1.78 \, \mu g \, m^{-3}$), Seoul ($1.52 \, \mu g \, m^{-3}$), and Gwangju ($1.13 \, \mu g \, m^{-3}$) in Korea (Yu et al., 2018). Despite the suburban location of Fukuoka, the BC ~~and ΔCO concentrations were~~ concentration was even lower than ~~those~~that of Baengnyeong~~,~~. However, the CO baseline concentration was highest among the measurement sites suggesting the influence of local sources, though it could be varied depending on geographical location. To check influence of local pollution at Fukuoka, we tested by applying more stringent CO baseline criteria (14-days moving 2 % percentile; ~166 ppbv). As a result, there was no significant changes in our results (less than -4 %). ~~indicating that the measurement site could not be seriously influenced by local sources.~~ In the case of Noto, the BC concentration was the lowest among the sites as $0.24 \, \mu g \, m^{-3}$. The concentration level was lower than the annual averages of $0.36 \, \mu g \, m^{-3}$ at Fukue (Kanaya et al., 2016) and $0.29 \, \mu g \, m^{-3}$ at Cape Hedo (Verma et al., 2011), which are regarded as background monitoring sites in Japan. The seasonal variation in the BC concentration at all sites showed similar patterns of being low in summer due to rainout followed by precipitation and increasing from fall due to house heating and/or crop biomass burning, along with the transition to westerly winds.

Figure 2 shows the time series of the BC, CO, ΔBC/ΔCO ratio and APTs at the Noto site. Regardless of precipitation during the measurement periods, the correlation coefficient (R) between BC and CO was 0.70 within the significance level ($p < 0.01$), indicating that BC and CO were emitted from similar sources. Additionally, the R between ΔBC/ΔCO and APT showed a slightly negative relationship as -0.24 within the significance level ($p < 0.01$), suggesting that the wet removal process removed BC, which resulted in a low ΔBC/ΔCO ratio. However, compared to Noto, the other sites showed weak negative relationships within the significance level ($p < 0.01$) because the amounts of APT at the other three sites were lower than that for Noto, which led to less distinctive wet removal effects (Table 2).

3.2 Regional variation in the ΔBC/ΔCO ratio

Figure 3 shows a comparison of the ΔBC/ΔCO ratio between the REAS emission inventories

16

and measured values at four sites. The solid symbols with error bars satisfy the fraction of frequency (> 5% in Figure S2) and the number of data for each bin ($N > 5$ in Figure S4). The open symbols with a dashed error bar were excluded from the analysis because they did not satisfy the criteria. It should be noted that the total number of data for dominant emission regions in this study was 2.7 times higher than that used by Kanaya et al. (2016), indicating significant improvement in the representativeness of the regional variation. Due to the large spatial variations in BC and CO in the REAS emission inventory depending on the dominant emission region, the coefficient of variation (CV; standard deviation divided by the mean) of the BC/CO ratio from the REAS emission inventory (0.65, over the six regions) was much higher than those from the measurements (0.09 – 0.13) at each site. The CV from the REAS emission inventory was still as high as 0.27 when the highest (South Korea) and the lowest ratios (North Korea) were excluded. Moreover, the BC/CO ratio from the REAS emission inventory was slightly higher than the measured ratios, except for North Korea, indicating that the REAS BC/CO ratio did not represent the real value. It should be noted that there were no significant changes in trends for the long-term variation of the ΔBC/ΔCO ratios of all sites, as well as BC/CO ratios from the Emissions Database for Global Atmospheric Research (EDGAR version 4.3.2; Crippa et al. 2018) emission inventory since 2008 and the MIX emission inventory (Li et al., 2017) in 2008 and 2010 (Figure S6). This result implied that comparison between the measurements and the REAS emission inventory was a reasonable approach, even though the time scale between them did not match. The differences in the ratios between the REAS and the measurements will be discussed further in section 3.3.

The ΔBC/ΔCO ratio in North China showed the lowest average value across China as 6.2 ± 0.5 ng m^{-3} ppb^{-1}, followed by East China (6.8 ± 0.3 ng m^{-3} ppb^{-1}) and Northeast China (7.9 ± 0.7 ng m^{-3} ppb^{-1}). The ratios of two or three regions in China showed significant differences at all sites when Welch's t-test or the ANOVA test was applied ($p < 0.05$), except for Baengnyeong. The lower ΔBC/ΔCO ratio in North China than in East China was also reported with 5.3 ± 2.1 and 6.4 ± 2.2 ng m^{-3} ppb^{-1} in Fukue, 7.0 ± 3.3 and 7.5 ± 4.6 ng m^{-3} ppb^{-1} in Cape Hedo, and 6.5 ± 0.4 and 8.8 ± 0.9 ng m^{-3} ppb^{-1} in Mt. Huang, respectively (Kanaya et al., 2016; Pan et al., 2011; Verma et al., 2011). In the case of Northeast China, the variation in the ratio over the measurement sites (0.09 of CV) was higher than that over other Chinese regions (0.07 and 0.04 of CV in East China and North China, respectively). The reason why a higher CV was observed even in the same emission source region is that the pathways of the backward

17

297 trajectories were different, depending on the measurement site (Figure ~~S5~~S7); the backward

298 trajectory of Noto passed over the eastern region (Heilongjiang), whereas that of Baengnyeong

299 passed over the western region of Northeast China (Liaoning). The information of Northeast

300 China emissions obtained from measurements at Gosan might have been more strongly

301 affected by emissions from South Korea than that at Baengnyeong (~~S4~~S5).

302   The mean $\Delta BC/\Delta CO$ ratios of North Korea and South Korea were similar as 7.3 and 7.8 $\pm$

303 1.2 ng m^{-3} ppb^{-1}, respectively. Verma et al. (2011) reported a lower ratio for the Korean

304 peninsula (both South and North Korea) as 5.7 ± 2.0 ng m^{-3} ppb^{-1}. It should be noted that the

305 $\Delta BC/\Delta CO$ ratios for South Korea estimated from observations at Korean and Japanese sites

306 were significantly different as 8.9 ± 5.3 ng m^{-3} ppb^{-1} and 6.7 ± 3.8 ng m^{-3} ppb^{-1}, respectively

307 ($p \leq 0.01$). These differences were also consistent with previous studies that reported ratios as

308 8.5 ng m^{-3} ppb^{-1} at Gosan (Sahu et al., 2009) and 6.7 ± 3.7 ng m^{-3} ppb^{-1} at Fukue (Kanaya et

309 al., 2016). This difference between the ratios could also be caused by the different influences

310 of the emission source regions, similar to the case in Northeast China. Baengnyeong and Gosan

311 were mainly influenced by the southwestern region of Korea, including the Seoul Metropolitan

312 Area (SMA), whereas the Fukuoka and Noto sites were mainly influenced by the southeastern

313 region of Korea (Figure ~~S6~~S8), suggesting large spatial variation in BC/CO over the Korean

314 peninsula. In the case of Japan, the mean $\Delta BC/\Delta CO$ ratio was 6.8 ± 0.2 ng m^{-3} ppb^{-1}, which

315 was higher than or similar to the reported values as 5.9 ± 3.4 ng m^{-3} ppb^{-1} at Fukue, 5.7 ± 0.9

316 ng m^{-3} ppb^{-1} at Tokyo and 6.3 ± 0.5 ng m^{-3} ppb^{-1} at Nagoya (Kondo et al., 2006; Kanaya et

317 al., 2016). Moreover, there were no significant differences in the $\Delta BC/\Delta CO$ ratio between Noto

318 and Fukuoka, although the trajectories passed through different regions of Japan (Figure ~~S7~~S9),

319 suggesting that the spatial variation in the $\Delta BC/\Delta CO$ ratio of Japan was smaller than that of

320 South Korea. The higher $\Delta BC/\Delta CO$ ratio of South Korea could be explained by the higher ratio

321 of diesel to gasoline vehicles in Korea (0.88) than in Japan (0.09) in 2015 (MLIT 2019; MOLIT

322 2019) because the BC/CO ratio from diesel vehicles is higher than that from gasoline vehicles

323 due to the different carbon atom contents (Zhou et al., 2009; Guo et al., 2017).

324

3.3 Comparison between the REAS v2.1 and measured $\Delta BC/\Delta CO$ ratios

326   In this section, we investigated the differences in $\Delta BC/\Delta CO$ between the measured values

327   and the REAS v2.1 emission inventory. We adopted the mean fractional bias (MFB, ranging

328   from -2 to 2) defined by

329    $$\text{MFB} = \frac{2}{N} \sum_{i=1}^{i=N} \frac{R_i - M_i}{R_i + M_i}$$ (1)

330   where R_i and M_i denote the REAS emission inventory and the measured ratio corresponding to

331   sample i, respectively.

332   East China showed the lowest MFB value among Chinese regions as 0.12, and the other two

333   regions had similar MFB values as 0.48 for North China and 0.35 for Northeast China,

334   indicating an overestimation of the REAS emission inventory in China. The BC/CO ratio from

335   the REAS emission inventory showed a higher ratio in North China (10.0 ng m^{-3} ppb^{-1}) than

336   in East China (7.7 ng m^{-3} ppb^{-1}), which is an opposite pattern to that of the measured ratios.

337   Considering that most trajectories passed Nei Mongol (12.5 ng m^{-3} ppb^{-1}) and Hebei (6.6 ng

338   m^{-3} ppb^{-1}) in North China with a lower measured ΔBC/ΔCO ratios, the BC/CO ratio in Nei

339   Mongol was likely overestimated. In Northeast China, the higher BC/CO ratio in Heilongjiang

340   (14.0 ng m^{-3} ppb^{-1} in REAS) than in Liaoning (11.3 ng m^{-3} ppb^{-1} in REAS) was consistent

341   with the tendency of the measured ΔBC/ΔCO ratio.

342   The BC/CO ratios from the REAS emission inventory for South Korea (23.2 ng m^{-3} ppb^{-1})

343   and North Korea (3.7 ng m^{-3} ppb^{-1}) were highly over- and underestimated, along with large

344   absolute values of MFB of 0.99 (by factor 3.0) and -0.66 (by factor 2.0), respectively. The

345   ΔBC/ΔCO ratio in South Korea was still found to be 9.6 ± 0.5 ng m^{-3} ppb^{-1} when the condition

346   was restricted to less than the 25th percentile of the maximum relative humidity during the

347   previous 72 hours (less than 67.2%) to ensure choosing cases without wet deposition effects.

348   Kanaya et al. (2016) pointed out that the industry and transport sectors could be the sources of

349   the large discrepancy between the REAS emission inventory and the measurements. Although

350   the ratio of the industry sector in South Korea (41.4 ng m^{-3} ppb^{-1}) is also much higher (13

351   times) than that in Japan, BC and CO from industrial emissions in South Korea only accounted

352   for 13.4% and 7.9% of the total, respectively. Here, we identify the relative importance of the

353   road transport sector; the BC/CO ratio from road transportation in South Korea was 26.8 ng

354   m^{-3} ppb^{-1}, which was 3.6 times higher than the ratio in Japan as 7.4 ng m^{-3} ppb^{-1}. Upon looking

355   more closely into the transportation sector, the BC/CO ratios from diesel vehicles were found

356 to be similar between S. Korea (120 ng m^{-3} ppb^{-1}) and Japan (109 ng m^{-3} ppb^{-1}), although the

357 BC emissions could vary depending on the installation of diesel particulate filters.

358 To easily compare the CO emission rates from gasoline vehicles between South Korea and

359 Japan, we roughly estimated the CO emission factor from gasoline vehicles. This hypothetical

360 CO emission factor was calculated by considering the actual mean daily mileages (31 and 12

361 km day^{-1} for South Korea and Japan, respectively), the actual number of gasoline vehicles in

362 2008 (MLIT 2016, 2019; MOLIT 2019; TS, 2009) and the total CO emission rates in the REAS

363 emission inventory; the hypothetical CO emission factor in Japan (15.8 CO g km^{-1}; 2.82 Tg

364 yr^{-1} from 40.8 million) was 6.9 times higher than that in Korea (2.3 CO g km^{-1}; 0.22 Tg yr^{-1}

365 from 8.3 million). Underestimation of the hypothetical CO emission factor in South Korea was

366 also observed in motorcycles (2.8 CO g km^{-1}; 0.06 Tg yr^{-1} from 1.8 million), which was lower

367 than that in Japan (14.7 g km^{-1}; 0.15 Tg yr^{-1} from 1.5 million), assuming the same motorcycle

368 mileages in South Korea. Clearly the hypothetical CO emission factor thus derived for Korea

369 is unlikely, pointing to underestimation of the assumed CO emission rate. We can roughly

370 revise the total CO emission rates (2.2 Tg) from gasoline vehicles (1.46 Tg) and motorcycles

371 (0.31 Tg) by applying the hypothetical CO emission factor of Japan. Although the hypothetical

372 CO emission factors had large uncertainties due to inaccurate mileages for gasoline vehicles

373 and motorcycles, the revised REAS BC/CO ratio decreased to 7.3 ng m^{-3} ppb^{-1}, which was

374 closer to that of the observations.

375 The recently updated Korean emission inventory Clean Air Policy Support System (CAPSS;

376 Lee et al. 2012; Yeo et al., 2019) based on 2015 also showed a high BC/CO ratio as 25.1 ng

377 m^{-3} ppb^{-1} (Table 3), with much lower hypothetical CO emission factors for gasoline vehicles

378 (1.1 CO g km^{-1}) and motorcycles (1.7 CO g km^{-1}) with similar mean mileage values (30.4 km

379 day^{-1}; TS, 2015), suggesting that BC and CO emissions still need to be improved. This high

380 BC/CO ratio (35.6 ng m^{-3} ppb^{-1}) was also found in the MIX emission inventory, whereas the

381 BC/CO ratio from the EDGAR inventory in 2010 was much closer to the measured ratio as

382 7.68 ng m^{-3} ppb^{-1}. Many researchers have been trying to improve the accuracy of the CO

383 emission rate in South Korea through the bottom-up emission inventory (0.90 Tg) and top-

384 down estimation (1.10 Tg) derived from the KORUS-AQ campaign (Table 3). However,

385 discrepancies still exist in not only the ΔBC/ΔCO ratio but also the CO emission rate. In

386 particular, the CO emission rate in South Korea showed large variations according to the

emission inventory, suggesting that CO emission rates over South Korea should be improved preferentially.

In the case of North Korea, the CO emission rate (5.14 Tg) from REAS was considerably higher than that of South Korea by a factor of 7.4 and was especially higher than that of Japan, resulting in a low BC/CO ratio as 3.7 ng m^{-3} ppb^{-1}. The domestic and industrial sectors in North Korea showed relatively low BC/CO ratios as 6.79 and 4.45 ng m^{-3} ppb^{-1}, respectively, compared to those in China (9.5 – 10.5 ng m^{-3} ppb^{-1} for industry and 13.9 – 15.6 ng m^{-3} ppb^{-1} for the domestic sector). The BC and CO emission rates were under- and/or overestimated, respectively, although the quality of fuel and/or end-of-pipe technology could be different. In addition, when we considered registered vehicles in North Korea (0.26 million) and South Korea (16.8 million), the CO emission from road transportation in North Korea (1.75 Tg) was similar to the roughly revised CO emission in South Korea (1.88 Tg), implying a highly overestimated CO emission rate for the transportation sector (Statics of Korea, 2017). The Comprehensive Regional Emissions inventory for Atmospheric Transport Experiment (CREATE; Woo et al., 2014) in 2015 and EDGAR reported much lower CO emission rates in North Korea (1.41 and 1.55 Tg, respectively). As a result, the BC/CO ratio from EDGAR falls within a reasonable range as 6.85 ng m^{-3} ppb^{-1}, indicating agreement with the measured ratio (7.3 ng m^{-3} ppb^{-1}). This is because the ratio in EDGAR CO emission rates relative to REAS rates (30% of REAS) was much smaller than that for EDGAR BC (56% of REAS; Table 3), especially in the road transportation (9% for CO and 21% for BC) and industry sectors (38% for CO and 51% for BC). Kim and Kim (2019) pointed out that the uncertainty in the REAS CO emission rate in North Korea could result from inaccurate emission factors for biofuel compared to fossil fuels because the REAS emission inventory included several biofuel sources (such as fuel wood, crop residue, and animal waste).

The mean ΔBC/ΔCO ratio in Japan showed good consistency between the REAS emission inventory (6.84 ng m^{-3} ppb^{-1}), along with lowest absolute MFB as -0.05, which was close to 0.09 from Kanaya et al. (2016). The BC and CO emission rates from EDGAR, MIX and ECLIPSE V5a were close to those from the REAS emission inventory, indicating that the BC and CO emission rates over Japan were more accurate than those over other regions (Table 3).

In the case of the MIX emission inventory, the emission rates from North and South Korea were derived from the REAS and CAPSS inventories, respectively, and both the emission rates

and BC/CO ratio were within a narrow range of those of the REAS inventory. However, for EDGAR, while the BC/CO ratios in North Korea, South Korea, and Japan were relatively consistent with the ratios from measurements, the overestimation for China was remarkable compared to both the measurement ratios and other emission inventories. Especially, North China showed the highest BC/CO ratio compared to East and Northeast China, because the industry sector in North China has the largest BC and CO emission rates (63% and 35% of total, respectively), along with a high BC/CO ratio (38.5 ng m^{-3} ppb^{-1}).

3.4 Seasonal variation in the ΔBC/ΔCO ratio

The regional ΔBC/ΔCO ratios in the previous sections might still contain variability because of spatial (differences in the pathways of trajectories) and/or temporal variation (differences in monthly emissions), even within the same dominant emission region. To explore this finer spatio-temporal variability in the ΔBC/ΔCO ratio, the monthly BC and CO emission rates in each grid (0.25° by 0.25°) in the REAS emission inventory were integrated over the pathway of the backward trajectory satisfying altitudes $\leq$ 2.5 km and were compared with the observations. Figure 4 shows the seasonal variation in the recalculated BC/CO ratios from the REAS emission inventory and the measured ΔBC/ΔCO ratios, regardless of the measurement sites.

The recalculated BC/CO ratios of China and North Korea showed similar seasonal variations, relatively high in winter and low in summer. This result was caused by the seasonal variation in the BC emission rate (CV: 0.11 – 0.17) being higher than that in the CO emission rate (CV: 0.07 – 0.14) according to REAS in China, and domestic heating is the main factor affecting the seasonality. In contrast, the seasonal pattern in the REAS BC/CO ratios of South Korea and Japan, higher in summer than in spring or winter, can be explained by the term of the CO emission rate (CV: 0.05 for South Korea and 0.12 for Japan) compared to that of BC (CV: 0.005 for South Korea and 0.03 for Japan), which showed a relatively constant rate throughout the year.

The average absolute MFB of ΔBC/ΔCO between the recalculated REAS and the measured values in all regions was 0.29, and that in spring was the lowest as 0.19, followed by winter (0.33), fall (0.34) and summer (0.61). However, the MFB in summer decreased to 0.30, which

was close to that in fall and winter, when the low $\Delta BC/\Delta CO$ ratio in North China and Northeast China was excluded due to the small number of data (≤ 50). The MFB in South Korea was too high, ranging from 0.64 to 0.93, due to underestimation of the CO emission rate, as discussed in section 3.3. It should be noted that the measured $\Delta BC/\Delta CO$ ratios in spring were the highest among the seasons for all dominant emission regions except for North Korea; in particular, those in East China, South Korea, and Japan showed significant differences in the $\Delta BC/\Delta CO$ ratios between spring and winter ($p \leq 0.05$). These higher $\Delta BC/\Delta CO$ ratios in spring than in winter were also observed at Hedo, Okinawa (Verma et al., 2011). This difference might be caused by the seasonality of BC emissions from the domestic sector between spring and winter, which was overwhelmed by the seasonality of CO emissions. The annual consumption of coal (high BC/CO ratios) for households was slightly decreased from 100.4 to 93.5 million tons, whereas that of natural gas (non-emitted BC) showed a significant increase from 7.9 to 36 billion m^3 as a factor of 3.6 times from 2005 to 2015 (National Bureau of Statistics of China, 2017). This fuel transition for the domestic sector could have caused a decreased $\Delta BC/\Delta CO$ ratio in winter due to the constant BC emission rate along with increasing CO emission rate.

Although the $\Delta BC/\Delta CO$ in Japan showed good agreement with the regional REAS BC/CO ratio, the mean absolute MFB was 0.30, which was not low, as we expected. In the REAS emission inventory, the CO emission rates in South Korea and Japan mainly varied due to the domestic sector and road transportation, respectively, and those rates were maximum in winter and minimum in summer. The reason why the observed $\Delta BC/\Delta CO$ ratios in both South Korea and Japan showed the highest values in spring and not summer is that the ratio of ΔBC in spring to that in summer was higher than the corresponding ratio of ΔCO, implying that seasonal variations in the CO emission rate could not represent the seasonal characteristics.

Similar to the regional variation, the seasonal variation of other inventories also showed large differences not only in the variation pattern but also in magnitude (Figure S10). As discussed for the regional variations of the emission inventory (section 3.3), the MIX inventory showed similar seasonal variations to those of the REAS emission inventory, indicating high BC/CO ratios in winter for China (due to residential heating) and high values in summer for Japan (due to traffic). On the other hand, the seasonal variation of EDGAR reached the maximum in summer for China and in winter for South Korea and Japan, which is an opposite seasonal pattern to that of the REAS and MIX emission inventories. The reason why the

23

3.5 Estimated potential regions of over- and underestimation for $\Delta BC/\Delta CO$

An investigation of the potential locations for over- and underestimated $\Delta BC/\Delta CO$ ratios was performed using a potential source contribution function (PSCF). Typically, the PSCF has been widely applied to identify source regions of aerosols on regional scales, as well as to identify long-range transported pollution to a receptor site (Guo et al., 2015; Kim et al., 2016). Unlike the grid size of the REAS emission inventory, the trajectory endpoints are assigned to cells of $0.5° \times 0.5°$ geographic coordinates with a latitude (i) and longitude (j), and the number of trajectory segment endpoints within the grid cell is counted. The PSCF at the ijth grid cell can be calculated by the following:

$$PSCF_{i,j} = \frac{\sum m_{i,j}}{\sum n_{i,j}}$$

where $n_{i,j}$ is the total number of trajectory endpoints over the ijth grid cell and $m_{i,j}$ is the number of these endpoints that correspond to values higher or lower than certain criteria over a certain grid cell. We applied MFB values higher than 0.5 and lower than -0.5 for over- and underestimated criteria, respectively. If the total number of trajectory segment endpoints in a particular cell ($\sum n_{i,j}$) is small, the PSCF value may be biased toward overestimation, especially when the value of $\sum m_{i,j}$ is higher at the receptor site. To reduce the effect of abnormal and large $PSCF_{ij}$ values with low $\sum n_{i,j}$, a weight function (Guo et al., 2015) was applied with the power law of the total number of trajectories ($N_{APT=0}$ for each site in Table 2).

For overestimated cases (MFB $\geq$ 0.5; Figure 5), South Korea was clearly identified as a region with a higher PSCF value, regardless of the measurement site. In particular, the western region of South Korea, including the SMA and the southwestern region, showed the highest PSCF values. High PSCF values in Baengnyeong were observed in the SMA region (17.2 ng

24

507 m^{-3} ppb^{-1} from REAS) with 0.60, whereas those in Gosan were located in the southwestern

508 region of Korea (30.7 ng m^{-3} ppb^{-1} from REAS) with 0.65, suggesting that the southwestern

509 region of Korea is more overestimated than the SMA region. Although the measured ΔBC/ΔCO

510 ratios were similar at Fukuoka and Noto, the overestimated region for Fukuoka was more

511 emphasized in SMA with a higher PSCF value (0.61) than that for Noto, which indicated that

512 the southeastern region (27.0 ng m^{-3} ppb^{-1} from REAS) had a relatively low PSCF (0.42). In

513 China, Liaoning (10.8 ng m^{-3} ppb^{-1} from REAS) in Northeast China revealed the highest PSCF

514 (0.43), followed by Tianjin (7.0 ng m^{-3} ppb^{-1} from REAS) in the North China at Baengnyeong,

515 along with similar results in Gosan. Fukuoka and Noto did not directly point out the

516 overestimation regions in China. Nonetheless, Noto may indicate that Heilongjiang (14.0 ng

517 m^{-3} ppb^{-1}) is related to a large overestimation of the ratio, as deduced from the pathway of

518 airmass toward Northeast China. For Japan, the Kyushu and central region (Kansai, Kanto, and

519 Chubu) showed moderate PSCF values (~0.3), implying relatively good consistency between

520 the REAS and the measured ratios.

521   On the other hand, a PSCF value higher than 0.2 for an underestimated case (MFB ≤ -0.5,

522 Figure 6) was observed only at the Baengnyeong site for North Korea. The most

523 underestimated regions were identified as the western regions of North Korea, such as

524 Pyongyang (4.72 ng m^{-3} ppb^{-1} from REAS) and nearby. These regions showed the highest CO

525 emission rates (Figure 1), especially from the industrial sector, suggesting that the accuracies

526 of the CO emission rates from not only road transportation but also the industrial sector should

527 be improved. The results of PSCF analysis provided useful information on the potentially over-

528 and underestimated BC/CO ratio regions where the BC and CO emission rates should be

529 preferentially updated.

530

531   **4 Conclusions**

532   To verify the REAS bottom-up emission inventory, the ΔBC/ΔCO ratios were diagnosed

533 from long-term, best-effort observations at four sites in East Asia, including two sites in Korea

534 (Baengnyeong and Gosan) and two sites in Japan (Fukuoka and Noto). Based on the backward

535 trajectories covering the past 72 hours, dominant emission regions were assigned to six study

536 domains divided by country and/or administrative district, including three Chinese regions

(East, North, and Northeast), two Korean peninsula regions (South and North Korea), and Japan. To choose cases without wet deposition effects, the $\Delta BC/\Delta CO$ ratio was considered only when the accumulated precipitation along a backward trajectory (APT) for three days was equal to zero.

The regional $\Delta BC/\Delta CO$ ratios were overestimated in the REAS emission inventory from East, North and Northeast China. The REAS BC/CO ratio of South Korea was 3.0 times higher than the measured $\Delta BC/\Delta CO$ ratio, whereas Japan showed good consistency between the two ratios. The plausible reason was that the CO emissions rates from gasoline vehicles and motorcycles in South Korea were highly underestimated when considering hypothetical CO emission factors compared to those in Japan. However, North Korea revealed a highly underestimated region by a factor of 2.0 due to unrealistically overestimated CO emissions from vehicles, although it is hard to directly compare these emissions with those in other countries due to the possibility of differences in fuel usage and combustion technology. The seasonal variation in the $\Delta BC/\Delta CO$ ratio revealed different tendencies. The BC/CO ratios from REAS (and MIX) peaked in winter (China and North Korea) and in summer (South Korea and Japan), which is an opposite seasonal pattern to that of EDGAR values. In contrast, the measured ratio was the highest in spring, implying that the REAS and other emission inventory inventories did not reflect the major seasonality driver. From the PSCF analysis, the potentially over- and underestimated regions were emphasized in the SMA and southwestern regions of South Korea and Pyongyang of North Korea, respectively. In addition to the highlighted regions in the Korean peninsula, moderate PSCF values for overestimation were also observed at Tianjin (East), Liaoning and Heilongjiang (Northeast) in China and at Kyushu and the central region in Japan.

This study provided the overall mean BC/CO ratio with uncertainty for each dominant emission region by taking into consideration the full range of the $\Delta BC/\Delta CO$ ratio based on spatial (four sites) and temporal variations (four seasons) (Table 3). The BC emissions over East Asia can be estimated by multiplying the observed $\Delta BC/\Delta CO$ ratio by reliable estimates of the CO emission rate. The discrepancy in the BC/CO ratio is largely contributed by inaccurate CO emission rates in emission inventories, in addition to BC emission factors. Therefore, to enhance the accuracy of the BC emission rate over East Asia, a comprehensive and in-depth investigation of CO emissions should be performed to accurately assess the CO

568 emission rate by considering not only the annual total but also the monthly basis, particularly

569 in the Korean peninsula.

570

Author contributions

572   YC and YK designed the study and prepared the manuscript with contributions from all co-

573 authors. SMP, HK and DHJ were responsible for measurements at Baengnyeong. AM and YS

574 conducted measurements at Noto and IU provided the data at Fukuoka. SWK and ML

575 contributed to ground observations and quality control at Gosan. XP contributed the data

576 analysis. All co-authors provided professional comments to improve the manuscript.

577

582

References

584 Bey, I., Jacob, D., Logan, J., and Yantosca, R.: Asian chemical outflow to the Pacific in
585   spring: Origins, pathways, and budgets, J. Geophys. Res.-Atmos., 106, 23097–23113,
586   doi:10.1029/2001JD000806, 2001

587 Bond, T. C., Anderson, T. L., and Campbell, D.: Calibration and Intercomparison of Filter-
588   Based Measurements of Visible Light Absorption by Aerosols, Aerosol Sci. Technol., 30,
589   582-600, 10.1080/027868299304435, 1999.

590 Bond, T. C., Doherty, S. J., Fahey, D., Forster, P., Berntsen, T., DeAngelo, B., Flanner, M.,
591   Ghan, S., Kärcher, B., and Koch, D.: Bounding the role of black carbon in the climate
592   system: A scientific assessment, J. Geophys. Res. Atmos., 118, 5380-5552, 2013.

593 Cho, C., Kim, S.-W., Lee, M., Lim, S., Fang, W., Gustafsson, Ö., Andersson, A., Park, R. J.,
594   and Sheridan, P. J.: Observation-based estimates of the mass absorption cross-section of
595   black and brown carbon and their contribution to aerosol light absorption in East Asia,
596   Atmos. Environ., 212, 65-74, https://doi.org/10.1016/j.atmosenv.2019.05.024, 2019.

597 Crippa, M., Guizzardi, D., Muntean, M., Schaaf, E., Dentener, F., van Aardenne, J. A.,
598   Monni, S., Doering, U., Olivier, J. G. J., Pagliari, V., and Janssens-Maenhout, G.: Gridded
599   emissions of air pollutants for the period 1970–2012 within EDGAR v4.3.2, Earth Syst.
600   Sci. Data, 10, 1987-2013, 10.5194/essd-10-1987-2018, 2018.

Draxler, R,. Stunder, B., Rolph, G., Stein, A., Taylor, A.: HYSPLIT4 user's guide, version 4, http://www.arl.noaa.gov/documents/reports/hysplit_user_guide.pdf, last access: 27 Jun 2019, 2018.

Geng, F., Hua, J., Mu, Z., Peng, L., Xu, X., Chen, R., and Kan, H.: Differentiating the associations of black carbon and fine particle with daily mortality in a Chinese city, Environmental Research, 120, 27-32, https://doi.org/10.1016/j.envres.2012.08.007, 2013.

Guo, Q., Hu, M., Guo, S., Wu, Z., Hu, W., Peng, J., Hu, W., Wu, Y., Yuan, B., Zhang, Q., and Song, Y.: The identification of source regions of black carbon at a receptor site off the eastern coast of China, Atmos. Environ., 100, 78-84, http://dx.doi.org/10.1016/j.atmosenv.2014.10.053, 2015.

Guo, Q., Hu, M., Guo, S., Wu, Z., Peng, J., and Wu, Y.: The variability in the relationship between black carbon and carbon monoxide over the eastern coast of China: BC aging during transport, Atmos. Chem. Phys., 17, 10395-10403, 10.5194/acp-17-10395-2017, 2017.

Han, S., Kondo, Y., Oshima, N., Takegawa, N., Miyazaki, Y., Hu, M., Lin, P., Deng, Z., Zhao, Y., Sugimoto, N., and Wu, Y.: Temporal variations of elemental carbon in Beijing, J. Geophys. Res. Atmos., 114, doi:10.1029/2009JD012027, 2009.

Han, K. M., Lee, S., Chang, L. S., and Song, C. H.: A comparison study between CMAQ-simulated and OMI-retrieved NO2 columns over East Asia for evaluation of NOx emission fluxes of INTEX-B, CAPSS, and REAS inventories, Atmos. Chem. Phys., 15, 1913-1938, https://doi.org/10.5194/acp-15-1913-2015, 2015.

Huebert, B. J., Bates, T., Russell, P. B., Shi, G., Kim, Y. J., Kawamura, K., Carmichael, G., and Nakajima, T.: An overview of ACE-Asia: Strategies for quantifying the relationships between Asian aerosols and their climatic impacts, J. Geophys. Res. Atmos., 108, doi:10.1029/2003JD003550, 2003.

Itahashi, S., Uno, I., Osada, K., Kamiguchi, Y., Yamamoto, S., Tamura, K., Wang, Z., Kurosaki, Y., and Kanaya, Y.: Nitrate transboundary heavy pollution over East Asia in winter, Atmos. Chem. Phys., 17, 3823-3843, 10.5194/acp-17-3823-2017, 2017.

Jacobson, M. Z.: Strong radiative heating due to the mixing state of black carbon in atmospheric aerosols, Nature, 409, 695, 10.1038/35055518.

Janssen, N., A. H., Hoek, G., Simic-Lawson, M., Fischer, P., van Bree, L., ten Brink, H., Keuken, M., Atkinson Richard, W., Anderson, H. R., Brunekreef, B., and Cassee Flemming, R.: Black Carbon as an Additional Indicator of the Adverse Health Effects of Airborne Particles Compared with PM10 and PM2.5, Environ. Health Perspect., 119, 1691-1699, 10.1289/ehp.1003369, 2011.

Janssen, N. A., Gerlofs-Nijland, M. E., Lanki, T., Salonen, R. O., Cassee, F., Hoek, G., Fischer, P., Brunekreef, B., and Krzyzanowski, M.: Health effects of black carbon, WHO Regional Office for Europe Copenhagen, 2012.

Kanaya, Y., Komazaki, Y., Pochanart, P., Liu, Y., Akimoto, H., Gao, J., Wang, T., and Wang, Z.: Mass concentrations of black carbon measured by four instruments in the middle of Central East China in June 2006, Atmos. Chem. Phys., 8, 7637-7649, 10.5194/acp-8-7637-2008, 2008.

Kanaya, Y., Taketani, F., Komazaki, Y., Liu, X., Kondo, Y., Sahu, L. K., Irie, H., and Takashima, H.: Comparison of Black Carbon Mass Concentrations Observed by Multi-Angle Absorption Photometer (MAAP) and Continuous Soot-Monitoring System (COSMOS) on Fukue Island and in Tokyo, Japan, Aerosol Sci. Technol., 47, 1-10, 10.1080/02786826.2012.716551, 2013.

Kanaya, Y., Pan, X., Miyakawa, T., Komazaki, Y., Taketani, F., Uno, I., and Kondo, Y.: Long-term observations of black carbon mass concentrations at Fukue Island, western Japan, during 2009–2015: constraining wet removal rates and emission strengths from East Asia, Atmos. Chem. Phys., 16, 10689-10705, 10.5194/acp-16-10689-2016, 2016.

Kim, B. M., Seo, J., Kim, J. Y., Lee, J. Y., and Kim, Y.: Transported vs. local contributions from secondary and biomass burning sources to PM2.5, Atmos. Environ., 144, 24-36, https://doi.org/10.1016/j.atmosenv.2016.08.072, 2016.

Kim, I. S., and Kim, Y. P.: Characteristics of Energy Usage and Emissions of Air Pollutants in North Korea, J. Korean Soc. Atmos. Environ., 35, 125-137, 2019.

Kondo, Y., Komazaki, Y., Miyazaki, Y., Moteki, N., Takegawa, N., Kodama, D., Deguchi, S., Nogami, M., Fukuda, M., Miyakawa, T., Morino, Y., Koike, M., Sakurai, H., and Ehara, K.: Temporal variations of elemental carbon in Tokyo, J. Geophys. Res. Atmos., 111, doi:10.1029/2005JD006257, 2006.

Kondo, Y., Sahu, L., Moteki, N., Khan, F., Takegawa, N., Liu, X., Koike, M., and Miyakawa, T.: Consistency and Traceability of Black Carbon Measurements Made by Laser-Induced Incandescence, Thermal-Optical Transmittance, and Filter-Based Photo-Absorption Techniques, Aerosol Sci. Tech., 45, 295-312, 10.1080/02786826.2010.533215, 2011.

Kondo, Y.: Effects of black carbon on climate: Advances in measurement and modeling, Monogr. Environ. Earth Planets, 3, 1-85, 2015.

Kurokawa, J., Ohara, T., Morikawa, T., Hanayama, S., Janssens-Maenhout, G., Fukui, T., Kawashima, K., and Akimoto, H.: Emissions of air pollutants and greenhouse gases over Asian regions during 2000–2008: Regional Emission inventory in ASia (REAS) version 2, Atmos. Chem. Phys., 13, 11019-11058, 10.5194/acp-13-11019-2013, 2013.

Li, M., Zhang, Q., Kurokawa, J. I., Woo, J. H., He, K., Lu, Z., Ohara, T., Song, Y., Streets, D. G., Carmichael, G. R., Cheng, Y., Hong, C., Huo, H., Jiang, X., Kang, S., Liu, F., Su, H., and Zheng, B.: MIX: a mosaic Asian anthropogenic emission inventory under the international collaboration framework of the MICS-Asia and HTAP, Atmos. Chem. Phys., 17, 935-963, 10.5194/acp-17-935-2017, 2017.

Lim, S., Lee, M., Lee, G., Kim, S., Yoon, S., and Kang, K.: Ionic and carbonaceous compositions of PM10, PM2.5 and PM1.0 at Gosan ABC Superstation and their ratios as source signature, Atmos. Chem. Phys., 12, 2007-2024, 10.5194/acp-12-2007-2012, 2012.

Loomis, D., Grosse, Y., Lauby-Secretan, B., Ghissassi, F. E., Bouvard, V., Benbrahim-Tallaa, L., Guha, N., Baan, R., Mattock, H., and Straif, K.: The carcinogenicity of outdoor air pollution, Lancet Oncol., 14, 1262-1263, https://doi.org/10.1016/S1470-2045(13)70487-X, 2013.

Matsui, H., Kondo, Y., Moteki, N., Takegawa, N., Sahu, L. K., Zhao, Y., Fuelberg, H. E., Sessions, W. R., Diskin, G., Blake, D. R., Wisthaler, A., and Koike, M.: Seasonal

variation of the transport of black carbon aerosol from the Asian continent to the Arctic during the ARCTAS aircraft campaign, Journal of Geophysical Research: Atmospheres, 116, 10.1029/2010JD015067, 2011.

Miyakawa, T., Oshima, N., Taketani, F., Komazaki, Y., Yoshino, A., Takami, A., Kondo, Y., and Kanaya, Y.: Alteration of the size distributions and mixing states of black carbon through transport in the boundary layer in east Asia, Atmos. Chem. Phys., 17, 5851-5864, 10.5194/acp-17-5851-2017, 2017.

Miyakawa, T., Kanaya, Y., Komazaki, Y., Taketani, F., Pan, X., Irwin, M., and Symonds, J.: Intercomparison between a single particle soot photometer and evolved gas analysis in an industrial area in Japan: Implications for the consistency of soot aerosol mass concentration measurements, Atmos. Environ., 127, 14-21, https://doi.org/10.1016/j.atmosenv.2015.12.018, 2016.

Miyazaki, K., Sekiya, T., Fu, D., Bowman, K. W., Kulawik, S. S., Sudo, K., Walker, T., Kanaya, Y., Takigawa, M., Ogochi, K., Eskes, H., Boersma, K. F., Thompson, A. M., Gaubert, B., Barre, J., and Emmons, L. K.: Balance of Emission and Dynamical Controls on Ozone During the Korea-United States Air Quality Campaign From Multiconstituent Satellite Data Assimilation, J. Geophys. Res. Atmos., 124, 387-413, doi:10.1029/2018JD028912, 2019.

MLIT (Ministry of Land, Infrastructure, Transport and Tourism): Annual report of Automobile transportation statistics in 2015, https://www.e-stat.go.jp/stat-search/file-download?statInfId=000031752810&fileKind=2, last access: 25 Jan 2019, 2016 (in Japanese).

MLIT: Traffic statistics book, http://www.mlit.go.jp/statistics/kotsusiryo.html, last access: 27 June 2019 (in Japanese).

MOLIT (Ministry of Land, Infrastructure and Transport): Total Registered Moter Vehicles, http://stat.molit.go.kr/portal/cate/statFileView.do?hRsId=58&hFormId=5..., last access: 8 Feb 2019 (in Korean).

Myhre, G., Shindell, D., Bréon, F.-M., Collins, W., Fuglestvedt, J., Huang, J., Koch, D., Lamarque, J.-F., Lee, D., and Mendoza, B., Nakajima, T., Robock, A., Stephens, G., Takemura, T., and Zhang, H.: Anthropogenic and Natural Radiative Forcing. In: Climate Change 2013: The Physical Science Basis. Contribution of Working Group I to the Fifth Assessment Report of the Intergovernmental Panel on Climate Change, Cambridge University Press, Cambridge, United Kingdom and New York, NY, USA, 2013.

Nakajima, T., Yoon, S.-C., Ramanathan, V., Shi, G.-Y., Takemura, T., Higurashi, A., Takamura, T., Aoki, K., Sohn, B.-J., Kim, S.-W., Tsuruta, H., Sugimoto, N., Shimizu, A., Tanimoto, H., Sawa, Y., Lin, N.-H., Lee, C.-T., Goto, D., and Schutgens, N.: Overview of the Atmospheric Brown Cloud East Asian Regional Experiment 2005 and a study of the aerosol direct radiative forcing in east Asia, J. Geophys. Res. Atmos., 112, doi:10.1029/2007JD009009, 2007.

National Bureau of Statistics of China: China Statistical Yearbook 2017, China Statistics Press, Beijing, ISBN-13: 978-7503782534, 2017.

NIOSH: Method 5040 issue 1: elemental carbon (diesel exhaust), 4th ed., Cincinnati, OH,

1996.

Ogren, J. A., Wendell, J., Andrews, E., and Sheridan, P. J.: Continuous light absorption photometer for long-term studies, Atmos. Meas. Tech., 10, 4805-4818, https://doi.org/10.5194/amt-10-4805-2017, 2017.

Ohara, T., Akimoto, H., Kurokawa, J., Horii, N., Yamaji, K., Yan, X., and Hayasaka, T.: An Asian emission inventory of anthropogenic emission sources for the period 1980–2020, Atmos. Chem. Phys., 7, 4419-4444, 10.5194/acp-7-4419-2007, 2007.

Ohata, S., Kondo, Y., Moteki, N., Mori, T., Yoshida, A., Sinha, P. R., and Koike, M.: Accuracy of black carbon measurements by a filter-based absorption photometer with a heated inlet, Aerosol Sci. Tech., 53, 1079-1091, 10.1080/02786826.2019.1627283, 2019.

Oshima, N., Kondo, Y., Moteki, N., Takegawa, N., Koike, M., Kita, K., Matsui, H., Kajino, M., Nakamura, H., Jung, J. S., and Kim, Y. J.: Wet removal of black carbon in Asian outflow: Aerosol Radiative Forcing in East Asia (A-FORCE) aircraft campaign, J. Geophys. Res. Atmos., 117, 10.1029/2011JD016552, 2012.

Pan, X. L., Kanaya, Y., Wang, Z. F., Liu, Y., Pochanart, P., Akimoto, H., Sun, Y. L., Dong, H. B., Li, J., Irie, H., and Takigawa, M.: Correlation of black carbon aerosol and carbon monoxide in the high-altitude environment of Mt. Huang in Eastern China, Atmos. Chem. Phys., 11, 9735-9747, 10.5194/acp-11-9735-2011, 2011.

Pan, X. L., Kanaya, Y., Wang, Z. F., Komazaki, Y., Taketani, F., Akimoto, H., and Pochanart, P.: Variations of carbonaceous aerosols from open crop residue burning with transport and its implication to estimate their lifetimes, Atmos. Environ., 74, 301-310, https://doi.org/10.1016/j.atmosenv.2013.03.048, 2013.

Park, R. J., Jacob, D. J., Palmer, P. I., Clarke, A. D., Weber, R. J., Zondlo, M. A., Eisele, F. L., Bandy, A. R., Thornton, D. C., Sachse, G.W., and Bond, T. C.: Export efficiency of black carbon aerosol in continental outflow: Global implications, J. Geophys. Res.-Atmos., 110, 1–7, https://doi.org/10.1029/2004JD005432, 2005.

Park, S.-S., Jung, S.-A., Gong, B.-J., Cho, S.-Y., and Lee, S.-J.: Characteristics of PM2.5 Haze Episodes Revealed by Highly Time-Resolved Measurements at an Air Pollution Monitoring Supersite in Korea, Aerosol Air Qual. Res., 13, 957-976, 10.4209/aaqr.2012.07.0184, 2013.

Petzold, A., Schloesser, H., Sheridan, P. J., Arnott, W. P., Ogren, J. A., and Virkkula, A.: Evaluation of Multiangle Absorption Photometry for Measuring Aerosol Light Absorption, Aerosol Sci. Technol., 39, 40-51, 10.1080/027868290901945, 2005.

Ramana, M. V., Ramanathan, V., Feng, Y., Yoon, S. C., Kim, S. W., Carmichael, G. R., and Schauer, J. J.: Warming influenced by the ratio of black carbon to sulphate and the black-carbon source, Nature Geoscience, 3, 542–545, , 2010.

Ramanathan, V., and Carmichael, G.: Global and regional climate changes due to black carbon, Nature Geoscience, 1, 221, 10.1038/ngeo156, 2008.

Sahu, L. K., Kondo, Y., Miyazaki, Y., Kuwata, M., Koike, M., Takegawa, N., Tanimoto, H., Matsueda, H., Yoon, S. C., and Kim, Y. J.: Anthropogenic aerosols observed in Asian continental outflow at Jeju Island, Korea, in spring 2005, J. Geophys. Res. Atmos., 114,

doi:10.1029/2008JD010306, 2009.

Saikawa, E., Kim, H., Zhong, M., Avramov, A., Zhao, Y., Janssens-Maenhout, G., Kurokawa, J.-I., Klimont, Z., Wagner, F., Naik, V., Horowitz, L. W., and Zhang, Q.: Comparison of emissions inventories of anthropogenic air pollutants and greenhouse gases in China, Atmos. Chem. Phys., 17, 6393–6421, https://doi.org/10.5194/acp-17-6393-2017, 2017.

Samset, B. H.: How cleaner air changes the climate, Science, 360, 148-150, 10.1126/science.aat1723, 2018.

Smith, K. R., Jerrett, M., Anderson, H. R., Burnett, R. T., Stone, V., Derwent, R., Atkinson, R. W., Cohen, A., Shonkoff, S. B., Krewski, D., Pope, C. A., Thun, M. J., and Thurston, G.: Public health benefits of strategies to reduce greenhouse-gas emissions: health implications of short-lived greenhouse pollutants, The Lancet, 374, 2091-2103, https://doi.org/10.1016/S0140-6736(09)61716-5, 2009.

Su, L., Yuan, Z., Fung, J. C. H., and Lau, A. K. H.: A comparison of HYSPLIT backward trajectories generated from two GDAS datasets, Sci. Total Environ., 506-507, 527-537, https://doi.org/10.1016/j.scitotenv.2014.11.072, 2015.

Statics of Korea: Major Statistics Indicators of North Korea, Statistics Korea, Korea, 287pp, 2017.

Taketani, F., Kanaya, Y., Nakayama, T., Ueda, S., Matsumi, Y., Sadanaga, Y., Iwamoto, Y., and Matsuki, A.: Property of Black Carbon Particles Measured by a Laser-Induced Incandescence Technique in the spring at Noto Peninsula, Japan, J. Aerosol Res., 31, 194-202, 10.11203/jar.31.194, 2016 (Abstract in English).

Turpin, B. J., Saxena, P., and Andrews, E.: Measuring and simulating particulate organics in the atmosphere: problems and prospects, Atmos. Environ., 34, 2983-3013, https://doi.org/10.1016/S1352-2310(99)00501-4, 2000.

TS (Korea Transportation Safety Authority): A research on the real condition of driving mileage in 2008, https://www.kotems.or.kr/app/kotems/forward?pageUrl=/kotems/ptl/bbs/KotemsPtlBbsStatsLs&topmenu1=06&topmenu2=03&topmenu3=03, last access: 25 Jun 2019, 2009 (In Korean).

TS: A research on the real condition of actual driving mileage in 2015 (2012-2015), https://www.kotems.or.kr/app/kotems/forward?pageUrl=/kotems/ptl/bbs/KotemsPtlBbsStatsLs&topmenu1=06&topmenu2=03&topmenu3=03, last access: 25 Jun 2019, 2016 (In Korean).

Ueda, S., Nakayama, T., Taketani, F., Adachi, K., Matsuki, A., Iwamoto, Y., Sadanaga, Y., and Matsumi, Y.: Light absorption and morphological properties of soot-containing aerosols observed at an East Asian outflow site, Noto Peninsula, Japan, Atmos. Chem. Phys., 16, 2525-2541, 10.5194/acp-16-2525-2016, 2016.

Uno, I., Osada, K., Yumimoto, K., Wang, Z., Itahashi, S., Pan, X., Hara, Y., Kanaya, Y., Yamamoto, S., and Fairlie, T. D.: Seasonal variation of fine- and coarse-mode nitrates and related aerosols over East Asia: synergetic observations and chemical transport model analysis, Atmos. Chem. Phys., 17, 14181-14197, 10.5194/acp-17-14181-2017, 2017.

809 Verma, R. L., Kondo, Y., Oshima, N., Matsui, H., Kita, K., Sahu, L. K., Kato, S., Kajii, Y.,
810   Takami, A., and Miyakawa, T.: Seasonal variations of the transport of black carbon and
811   carbon monoxide from the Asian continent to the western Pacific in the boundary layer, J.
812   Geophys. Res. Atmos., 116, doi:10.1029/2011JD015830, 2011.

813 Wang, Y., Wang, X., Kondo, Y., Kajino, M., Munger, J. W., and Hao, J.: Black carbon and its
814   correlation with trace gases at a rural site in Beijing: Top-down constraints from ambient
815   measurements on bottom-up emissions, J. Geophys. Res. Atmos., 116,
816   doi:10.1029/2011JD016575, 2011.

817 Woo, J.-H., Choi, K.-C., Kim, H. K., Baek, B. H., Jang, M., and Eum, J.-H.: Development of
818   an anthropogenic emissions processing system for Asia using SMOKE. Atmos. Environ.,
819   58, 5-13, 2012.

820 Woo, J.-H., Quan, S., Choi, K.-C., Kook, H., Jin, H., Song, C.-K., Han, J., and Lee, S.:
821   Development of the CREATE inventory in support of integrated modeling of climate and
822   air quality for East Asia, GEIA Conference, Boulder, USA, 2014.

823 Yeo, S.-Y., Lee, H.-K., Choi, S.-W., Seol, S.-H., Jin, H.-A., Yoo, C., Lim, J.-Y., and Kim, J.-
824   S.: Analysis of the National Air Pollutant Emission Inventory (CAPSS 2015) and the
825   Major Cause of Change in Republic of Korea, Asian J. Atmos. Environ., 13, 212-231,
826   2019.

827 Yu, G. H., Park, S. S., Ghim, Y. S., Shin, H. J., Lim, C. S., Ban, S. J., Yu, J. A., Kang, H. J.,
828   Seo, Y. K., Kang, K. S., Jo, M. R., Jung, S. A., Lee, M. H., Hwang, T. K., Kang, B. C.,
829   and Kim, H. S.: Difference in Chemical Composition of PM2.5 and Investigation of its
830   Causing Factors between 2013 and 2015 in Air Pollution Intensive Monitoring Stations, J.
831   Korean Soc. Atmos. Environ., 34, 16-37, 2018.

832 Zhou, X., Gao, J., Wang, T., Wu, W., and Wang, W.: Measurement of black carbon aerosols
833   near two Chinese megacities and the implications for improving emission inventories,
834   Atmos. Environ., 43, 3918-3924, https://doi.org/10.1016/j.atmosenv.2009.04.062, 2009.

835 Zhu, C., Kanaya, Y., Yoshikawa-Inoue, H., Irino, T., Seki, O., and Tohjima, Y.: Sources of
836   atmospheric black carbon and related carbonaceous components at Rishiri Island, Japan:
837   The roles of Siberian wildfires and of crop residue burning in China, Environ. Pollut.,
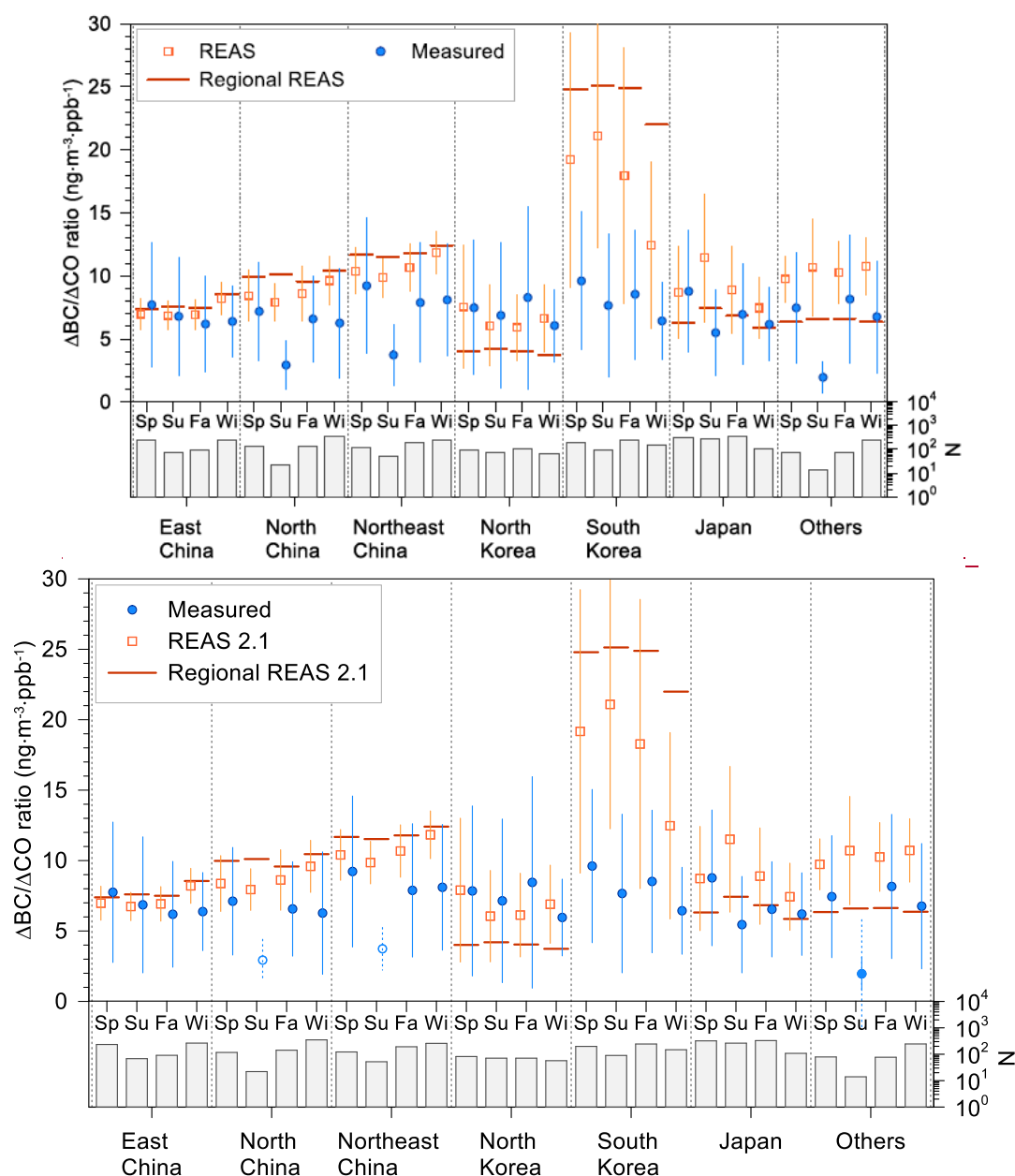838   247, 55-63, https://doi.org/10.1016/j.envpol.2019.01.003, 2019.
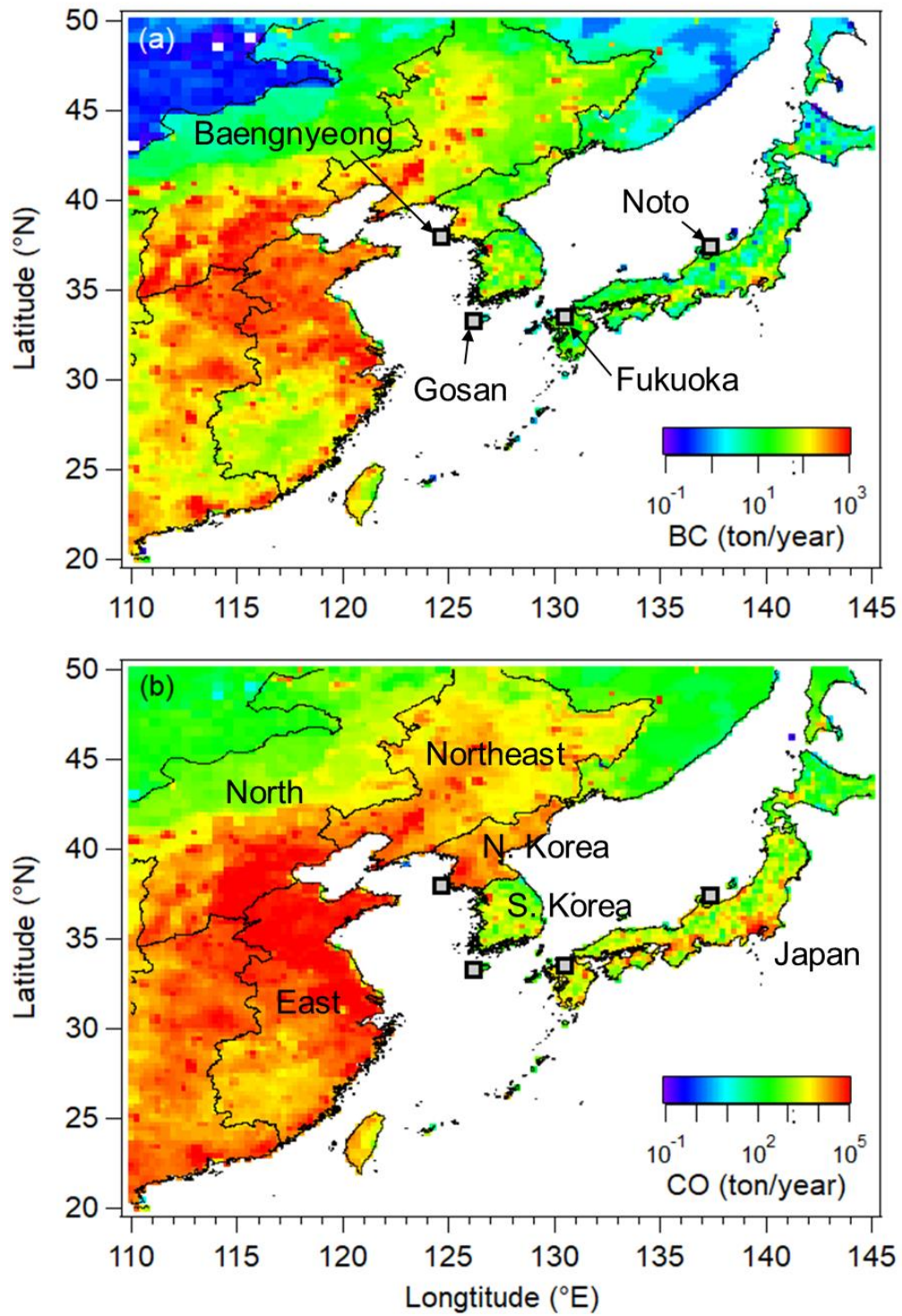
Figure 1. Yearly (a) BC and (b) CO emission rates (ton/year) over East Asia in 2008 from the REAS 2.1 bottom-up emission inventory (Kurokawa et al., 2013). The four measurement sites are shown in (a). (b) shows that the six study domains are divided by country and/or administrative district, including three Chinese regions (East, North, and Northeast), two Korean peninsula regions (South and North Korea), and Japan.
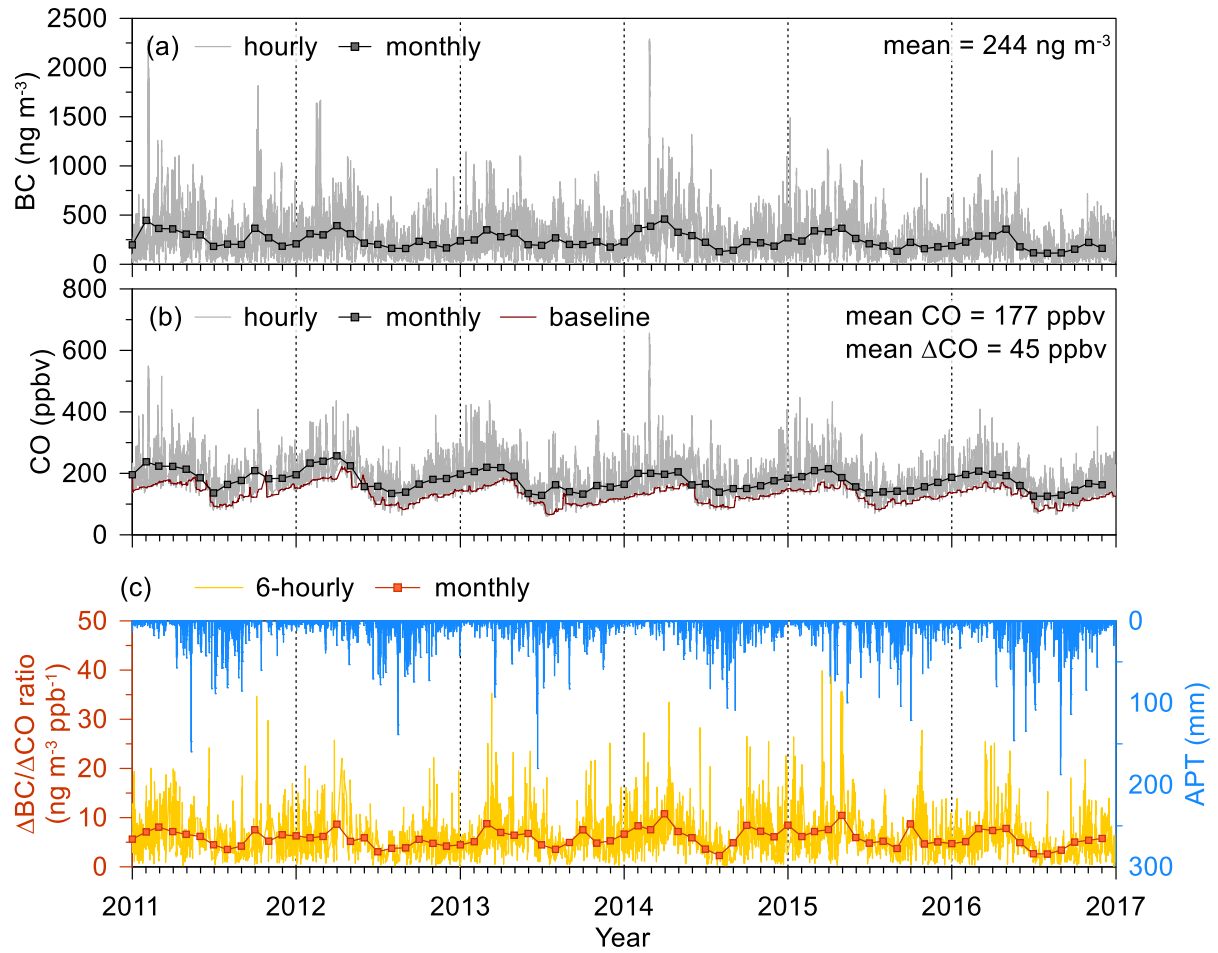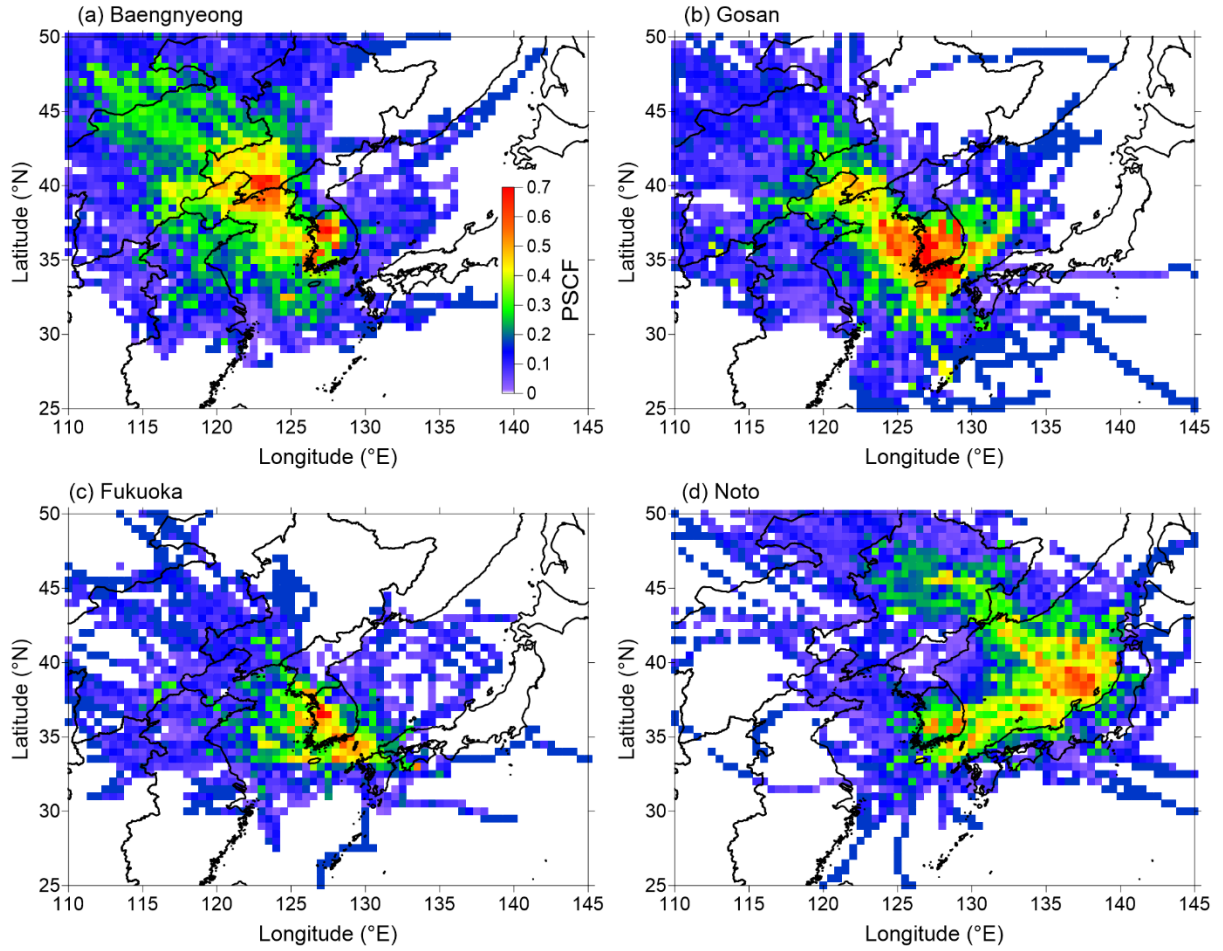
Figure 2. Time series of (a) BC concentration, (b) CO and ΔCO concentrations and (c) ΔBC/ΔCO ratio and accumulated precipitation along with trajectory (APT), during the measurement periods (from 2011 to 2017) in Noto, Japan. The square symbols with solid lines in (a) and (b) indicate hourly and monthly concentrations.
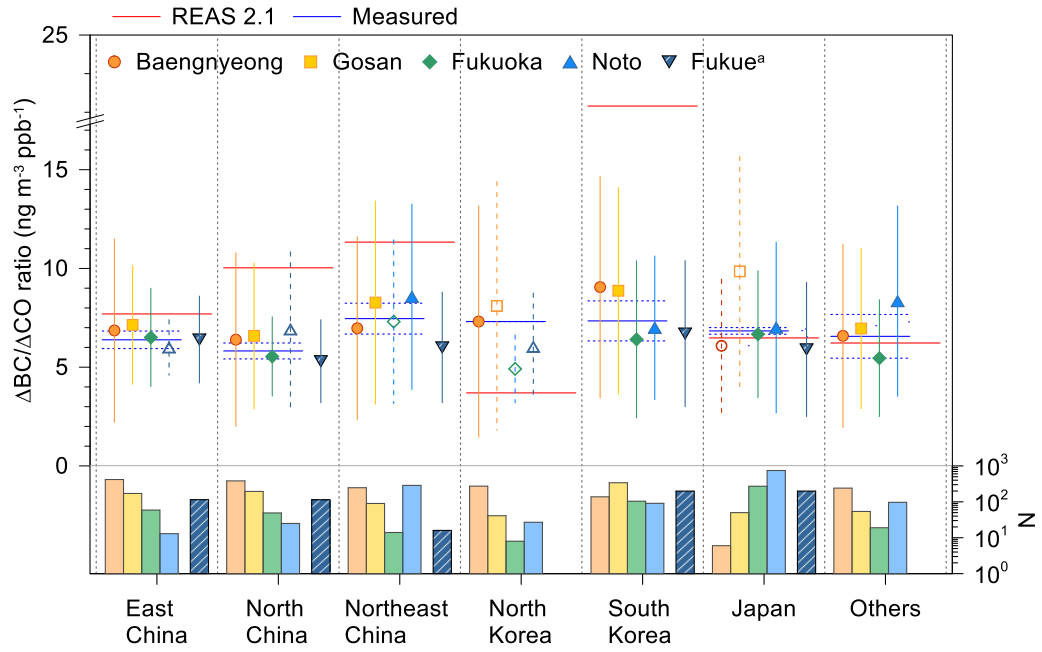
Figure 3. ΔBC/ΔCO ratios at the four measurement sites and Fukue from Kanaya et al. (2016) according to the dominant emission region. The symbols with vertical lines are the means and standard deviations of the ΔBC/ΔCO ratio. The bar graph on the bottom indicates the number of data in the dominant emission region. Open symbols with dashed vertical lines indicate data excluded because of a low number of data. The solid blue horizontal lines with dashed lines for each region indicate the means and standard deviations of the measured ΔBC/ΔCO, excluding the areas with limited data. The solid red horizontal lines depict the overall mean BC/CO ratios of dominant emission regions from the REAS version 2.1 emission inventory (Kurokawa et al., 2013).

Figure 4. The seasonal ΔBC/ΔCO ratios from four measurement sites (filled blue circles) and recalculated REAS BC/CO ratios according to the pathway of the trajectory (open orange squares), depending on the dominant emission region. The symbols with vertical lines are the means and standard deviations of the ΔBC/ΔCO ratios. Open-circle symbols with dashed vertical lines indicate data excluded because of a low number of data (≤ 50). The horizontal lines for each region indicate the overall mean values of the ΔBC/ΔCO ratios of dominant emission regions from the REAS version 2.1 emission inventory (Kurokawa et al., 2013). The bar graph on the bottom indicates the number of data in each season and the dominant emission region. The symbols with vertical lines are the means and standard deviations of the ΔBC/ΔCO ratios. The abbreviation of 'Sp' to 'Wi' indicates spring to winter.

Figure 5. Spatial distribution of the PSCF results for the mean fractional bias (MFB) ≥ 0.5 for overestimation cases at the (a) Baengnyeong, (b) Gosan, (c) Fukuoka, and (d) Noto sites. MFB is calculated from $2 \times (R_i - M_i)/(R_i + M_i)$, where R_i and M_i denote the mean values of the recalculated REAS BC/CO ratio along with the backward trajectory and the measured BC/CO ratio, respectively.
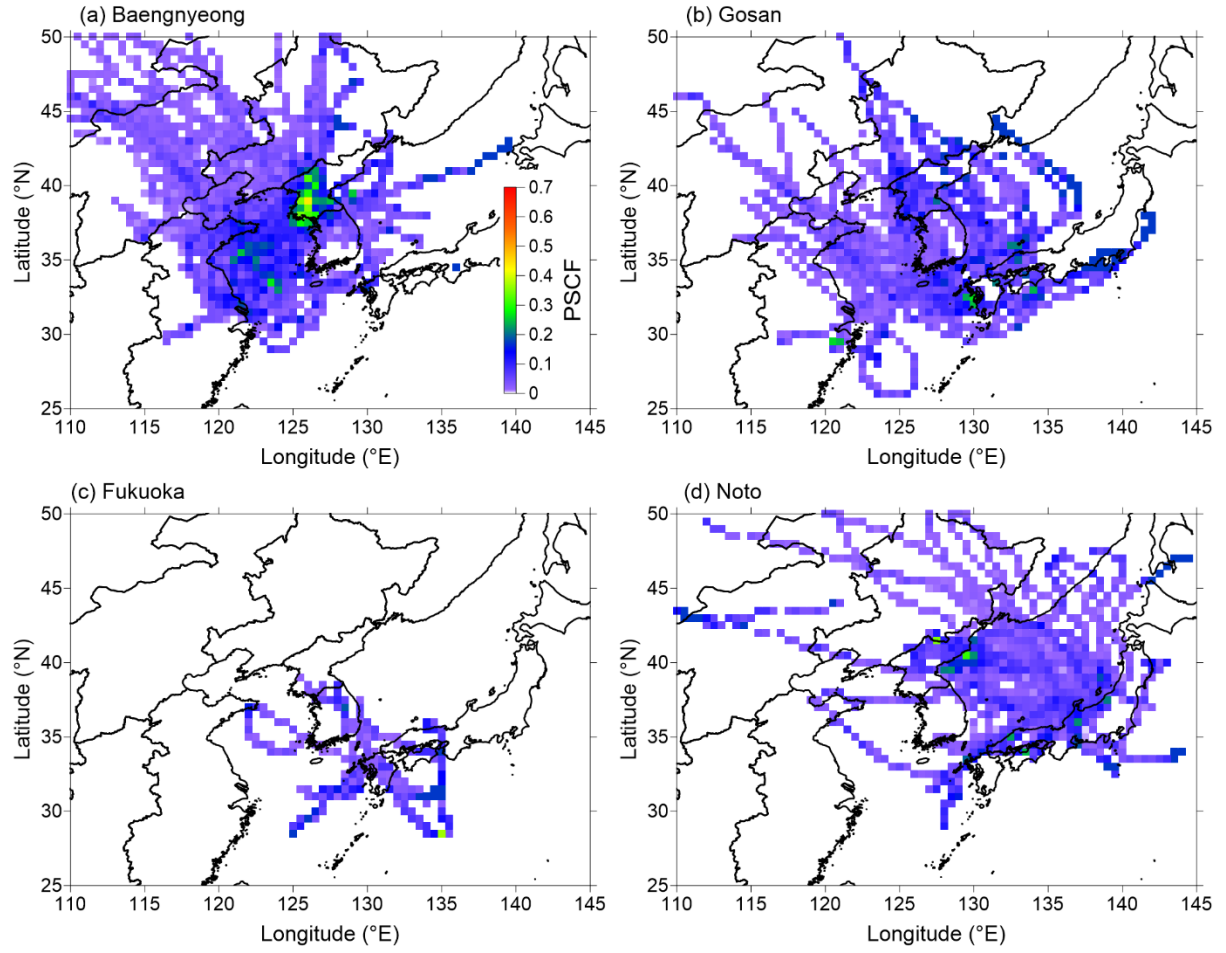
Figure 6. Same as Figure 5, except for the mean fractional bias (MFB) ≤ -0.5 for underestimation cases.

Table 1. Description of the measurement sites, periods, and instruments.

Sites		Longitude, Latitude	Measurement periods	Instruments
South Korea	Baengnyeong (background)	124.63 °E, 37.97 °N	2010.01.01 – 2016.12.31 (except for 2011 and 2012)	EC: sunset EC/OC (PM$_{2.5}$) CO: Teledyne API 300E
	Gosan (background)	126.17 °E, 33.28 °N	2012.05.01 – 2015.4.30	BC: CLAP[a] (PM$_1$) CO: Model 48i
Japan	Noto (background)	137.36 °E, 37.45 °N	2011.01.01 – 2016.12.31	BC: MAAP[b] (PM$_{2.5}$) CO: Model 48i
	Fukuoka (suburban area)	130.47 °E, 33.52 °N	2014.09.01 – 2016.03.31	BC: MAAP (PM$_{2.5}$) CO: Model 48i

[a] continuous light absorption photometer, [b] multi-angle absorption photometer

Table 2. Means and standard deviations of the black carbon (BC)[a], carbon monoxide (CO)[b], ΔCO concentrations[b], CO baseline[b], amount of APT[c] and the number of data for all (N_{all}) and APT=0 ($N_{APT=0}$) cases at each site.

	All	Spring	Summer	Fall	Winter
(a) Baengnyeong					
BC	826.5 ± 304.4	855.8 ± 204.0	561.7 ± 149.7	795.3 ± 300.8	1017.9 ± 347.2
CO	293.8 ± 63.8	317.4 ± 40.0	242.6 ± 46.2	264.5 ± 59.8	339.0 ± 57.9
ΔCO	128.9 ± 46.5	121.1 ± 24.0	104.1 ± 48.7	116.8 ± 41.7	167.4 ± 43.1
$CO_{baseline}$	164.9 ± 43.1	196.3 ± 25.9	138.6 ± 46.1	147.7 ± 40.0	171.6 ± 36.7
APT	3.6 ± 9.1	2.8 ± 6.4	9.1 ± 16.1	2.8 ± 6.5	1.5 ± 3.7
N_{All}	3,828	1,155	764	669	1,240
$N_{APT=0}$	1,793	560	199	339	695
(b) Gosan					
BC	490.2 ± 168.4	659.4 ± 200.4	323.4 ± 92.3	454.6 ± 59.7	542.2 ± 94.8
CO	190.1 ± 49.5	225.9 ± 20.0	128.4 ± 38.5	178.9 ± 29.4	227.1 ± 23.2
ΔCO	81.6 ± 27.2	87.2 ± 15.9	53.8 ± 21.3	77.8 ± 22.2	107.7 ± 18.8
$CO_{baseline}$	108.4 ± 29.4	138.7 ± 6.7	74.6 ± 28.2	101.0 ± 17.8	119.4 ± 9.7
APT	6.4 ± 14.4	4.2 ± 10.3	15.1 ± 23.0	5.2 ± 10.5	1.8 ± 3.6
N_{All}	2,510	395	598	778	739
$N_{APT=0}$	950	185	100	343	322
(c) Fukuoka					
BC	676.5 ± 105.8	665.5 ± 73.4	571.4 ± 43.9	700.0 ± 157.6	715.0 ± 63.3
CO	305.7 ± 43.7	303.6 ± 27.0	251.6 ± 34.7	293.3 ± 36.1	346.5 ± 26.8
ΔCO	124.6 ± 33.3	100.0 ± 22.9	99.6 ± 7.0	125.3 ± 35.4	152.9 ± 24.2
$CO_{baseline}$	181.1 ± 22.7	203.6 ± 5.0	151.9 ± 28.3	168.1 ± 8.8	193.6 ± 11.9
APT	6.4 ± 13.4	7.2 ± 13.7	13.9 ± 20.5	6.0 ± 13.1	3.3 ± 7.5

N_{All}	1,435	286	206	427	516
$N_{APT=0}$	547	114	37	179	217
(d) Noto					
BC	244.6 ± 81.0	339.9 ± 45.3	201.7 ± 54.2	203.1 ± 57.7	233.6 ± 74.6
CO	176.9 ± 31.9	212.1 ± 17.9	148.4 ± 17.1	157.2 ± 20.4	189.9 ± 21.7
ΔCO	45.4 ± 10.7	48.9 ± 7.4	44.8 ± 11.9	42.0 ± 10.9	46.2 ± 11.7
$CO_{baseline}$	131.4 ± 28.0	163.3 ± 16.2	103.6 ± 17.0	115.2 ± 12.8	143.7 ± 15.0
APT	7.9 ± 14.6	7.2 ± 13.9	13.7 ± 20.3	7.9± 13.4	3.2 ± 4.3
N_{All}	6,089	1,482	1,468	1,574	1,565
$N_{APT=0}$	1,290	415	267	353	255

[a] ng m^{-3}; [b] ppbv; [c] mm

Table 3. (a) Regional $\Delta BC/\Delta CO$ (ng m^{-3} ppb^{-1}) ratios and emission rates of (b) BC and (c) CO (in Tg per year) over East Asia from various emission inventories.

	This study[a]	REAS 2.1 (2008)	EDGAR (2010)	MIX (2010)	CAPSS (2015)	ECLIPSE (2015)	KORUS V2[c] (2016)	QA4ECV[d] (2016)
(a) $\Delta BC/\Delta CO$								
East China	6.8 ± 0.5	7.70	13.5	11.7		10.6		
North China	6.4 ± 0.5	10.0	21.1	12.8		13.4		
Northeast China	8.2 ± 0.7	11.8	12.9	11.9		13.2		
North Korea	7.2 ± 0.7	3.70	6.85	3.90	-	21.1		
South Korea	7.9 ± 1.2	23.2	7.68	35.6	25.1	10.6	17.8[e]	14.5[e]
Japan	6.8 ± 1.0	6.48	7.27	5.87	-	6.44		
(b) BC								
East China		0.400	0.329[b]	0.416		0.382[b]		
North China		0.331	0.215[b]	0.360		0.355[b]		
Northeast China		0.157	0.142[b]	0.158		0.181[b]		
North Korea		0.015	0.009	0.014	-	0.056[b]	-	
South Korea		0.013	0.016	0.024	0.016	0.027[b]	-	
Japan		0.026	0.023	0.020	-	0.019[b]	-	
(c) CO								
East China		65.0	30.5[b]	44.4		45.2		
North China		41.2	12.7[b]	35.1		33.1		
Northeast China		16.6	13.8[b]	16.6		17.1		
North Korea		5.14	1.55	4.49	-	3.30		
South Korea		0.69	2.56	0.84	0.79	3.18	0.90	1.10
Japan		5.03	3.97	4.28	-	3.66		

[a] With uncertainty (1σ) calculated by regional and seasonal mean values.
[b] Calculated based on administrative division from the emission inventory, which did not provide regional emission rates.
[c] Based on the improved CAPSS for 2015 and CREATE v3 in China for 2015 using SMOKE-Asia emission processing at a 0.1° resolution

(Woo et al., 2012).

[d] From multiconstituent data assimilation. Please find more details in Miyazaki et al. (2019).

[e] Using the BC emission rate from the REAS 2.1 emission inventory

Regional variability in black carbon and carbon monoxide ratio from long-term observations over East Asia: Assessment of representativeness for BC and CO emission inventories

Yongjoo Choi et al.

Correspondence to: Yongjoo Choi (choingjoo@jamstec.go.jp)

S1 Seasonal variation in dominant emission regions

Figure S2 shows the seasonal variation in data frequency and total mean fraction of dominant emission regions when APT was zero (without precipitation). Depending on the geographical characteristics, there is a distinct pattern of dominant emission regions. We decided that the valid dominant emission regions would only be considered when the fraction of frequency was higher than 5% to ensure an adequate statistical analysis. As a result, Baengnyeong was suitable for monitoring the Chinese regions (East, North, and Northeast; 14–25%) and Korea (South and North; 8.1% and 16%, respectively), whereas Gosan was mainly influenced by the Chinese regions (11–20%) and South Korea (37%), along with a decreasing fraction of North Korea (4.2%). The Fukuoka and Noto sites were also good representatives for emissions from Japan (51% and 58%, respectively); however, Fukuoka was good for East and North China (12% and 9.3%) and South Korea (20%), and Noto was good for Northeast China (22%) and South Korea (7.1%).

S2 Dry deposition effects

The basic assumption in this analysis is that the BC concentration does not show a significant decrease due to dry deposition during transport from the main source region. Similar to Kanaya et al. (2016), we investigated the effect of dry deposition on BC particles from the main source regions to the receptor sites. Figure S3 is an example of a scatter plot between the $\Delta BC/\Delta CO$ ratio and traveling time at the Noto site, with the mean value of each five-hour bin less than 72 hours. The slope of the exponential best fit line is very low as $1.32 \pm 1.88 \times 10^{-3}$ hour^{-1} (mean $\pm$ 95% confidence interval) which is correspondence to 0.02 cm s^{-1} for the mean and 0.06 cm s^{-1} for the upper 95% confidence interval of dry deposition velocities when the mean mixing height was 646 m, as calculated by the HYSPLIT model. Not only the Noto site but also the other three sites also showed low dry deposition velocities within a range between 0.01 and 0.03 cm s^{-1}, suggesting that the assumption is valid.

S3 The variation in the ΔBC/ΔCO ratio depends on the residence time

Since the ΔBC/ΔCO ratio could be influenced by the residence time over the emission source regions, it should be investigated whether the variation in the ΔBC/ΔCO ratio depends on the residence time in the same dominant emission region. Figure S4 shows the mean ratio with the standard deviation (vertical solid lines) divided by 20% intervals of the residence time fraction (total 73 hours) of the dominant emission region, along with a bar plot, which indicates the number of data for each bin. The open square symbols with a vertical dashed line indicate that the number of data was less than five (the 25th percentile of the number of data in each bin). We found that ΔBC/ΔCO did not vary significantly according to the fraction of residence time when the number of data (N) was higher than five. The difference between each fraction in the same dominant emission region was statistically insignificant ($p > 0.05$), except for 'South Korea' in Fukuoka and 'Others' in Noto, when Welch's t-test and the analysis of variance (ANOVA) were applied to two and more than two groups, respectively. This result indicated that the variation in the ΔBC/ΔCO ratio according to the fraction (residence time) could be negligible when N exceeds five for the fraction of the residence time. Hereafter, we used the data that satisfied the threshold ($N > 5$) of each bin for comparison with the REAS emission inventory. To verify whether these results were caused by the influences of other emission regions, the dominant emission region was constrained by considering only direct influences without passing through other emission regions. Although the constrained ΔBC/ΔCO ratios were only available for Korea and Japan, the mean ratios did not show a significant difference from the original ratio, implying that the effects of other emission regions were not significant.

~~S4~~S4 Uncertainty of regional and seasonal ΔBC/ΔCO ratios

The ΔBC/ΔCO ratio could be influenced by applying difference estimation methods for the CO baseline and altitude criteria for allocation of the dominant emission region. First, there are several ways to determine the CO baseline, mainly depending on the measurement period. For intensive measurement periods, the CO baseline can be calculated from the 5th percentile of data (Matsui et al. 2011; Miyakawa et al., 2017) or the x-intercept of the best-fit line between BC and CO (Oshima et al., 2012). It can also be calculated by the 5th percentile of the CO concentration from monthly (Verma et al. 2011) or moving 14-day (Kanaya et al. 2016) from long-term measurements. We tested the difference in CO baselines calculated from the 5th

percentile of the moving 14-day (our method) and monthly CO data (Figure S5). The difference in the CO baseline from the monthly data was slightly lower (-2 ppbv; -1.9%) than our estimation. Moreover, the mean $\Delta BC/\Delta CO$ ratios from the two different methods did not show significant differences (5.82 ng m^{-3} ppb^{-1} for our estimation and 5.87 ng m^{-3} ppb^{-1} for monthly data), when Welch's t-test was applied ($p > 0.1$). Second, we also checked the difference in $\Delta BC/\Delta CO$ which can be caused by applying 1.5 km as a threshold to determine the dominant emission region. There was no significant difference in the regional $\Delta BC/\Delta CO$ ratios between 2.5 and 1.5 km when Welch's t-test was applied ($p \geq 0.1$). For the seasonal variation, though five cases (spring, fall and winter in East China, fall in North China and winter in Northeast China) of recalculated REAS BC/CO values showed significant differences ($p < 0.05$), the ratios of those cases varied within $\pm$ 1.4 ng m^{-3} ppb^{-1} ($\pm$ 15%), indicating that the MFBs were preserved. From these results, we confirmed the representativeness of our regional and seasonal $\Delta BC/\Delta CO$ analysis.

S5 Footprint for Northeast China

Although the backward trajectory for Gosan passed a similar region to that for Baengnyeong (Figure S5S7) and the difference in the $\Delta BC/\Delta CO$ ratio due to residence time was negligible, it was hard to exclude the possibility of mixing with emissions from South Korea from the beginning. The high $\Delta BC/\Delta CO$ in the low-residence time fraction for Northeast China in Gosan also supported the possibility of influence from South Korea (Figure S4).
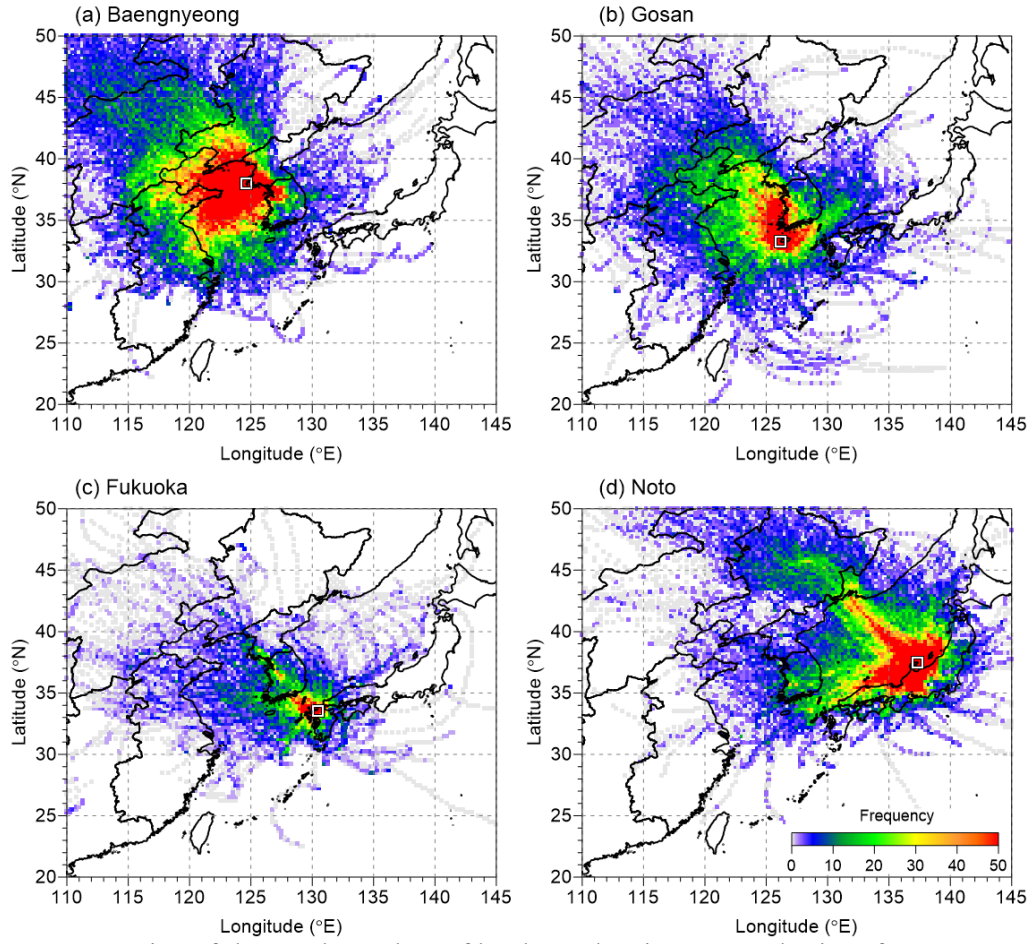
Figure S1. Footprint of the total number of backward trajectory endpoints for a 0.5°×0.5° grid cell depending on the measurement site.
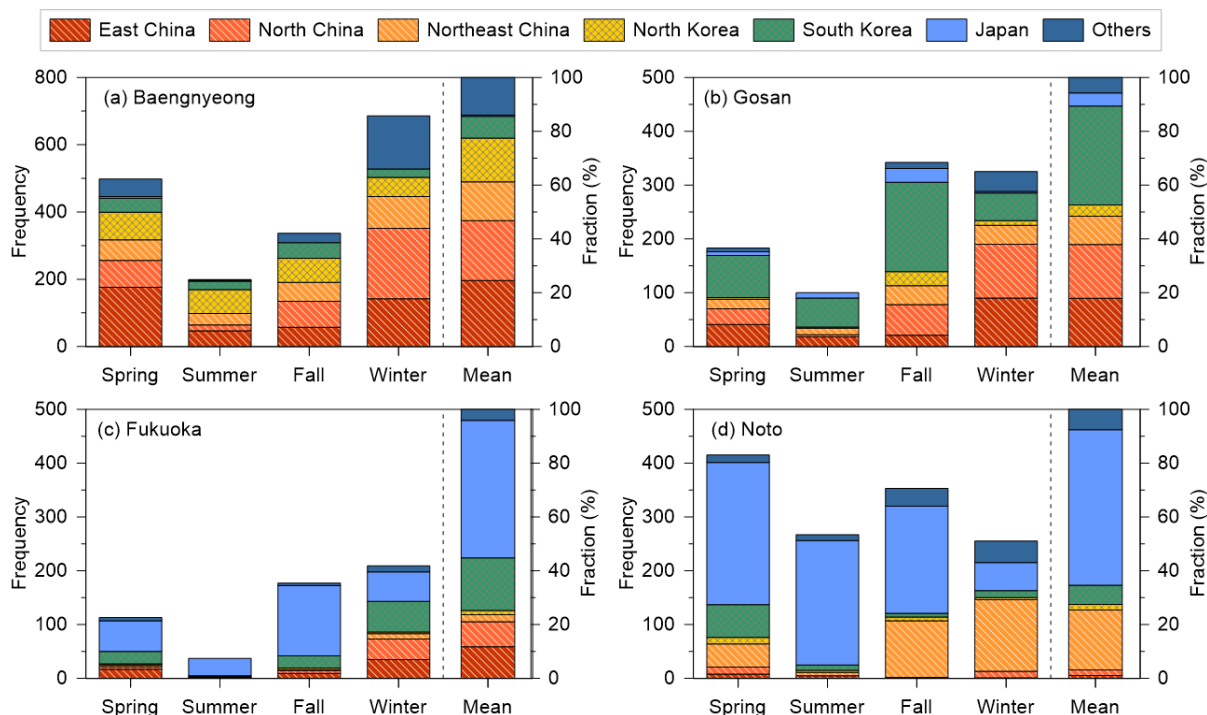
Figure S2. Seasonal variation in the frequency (left side of the dashed lines) and fraction (right side of the dashed lines) for backward trajectory-passed areas (dominant emission regions) in (a) Baengnyeong, (b) Gosan, (c) Fukuoka and (d) Noto.
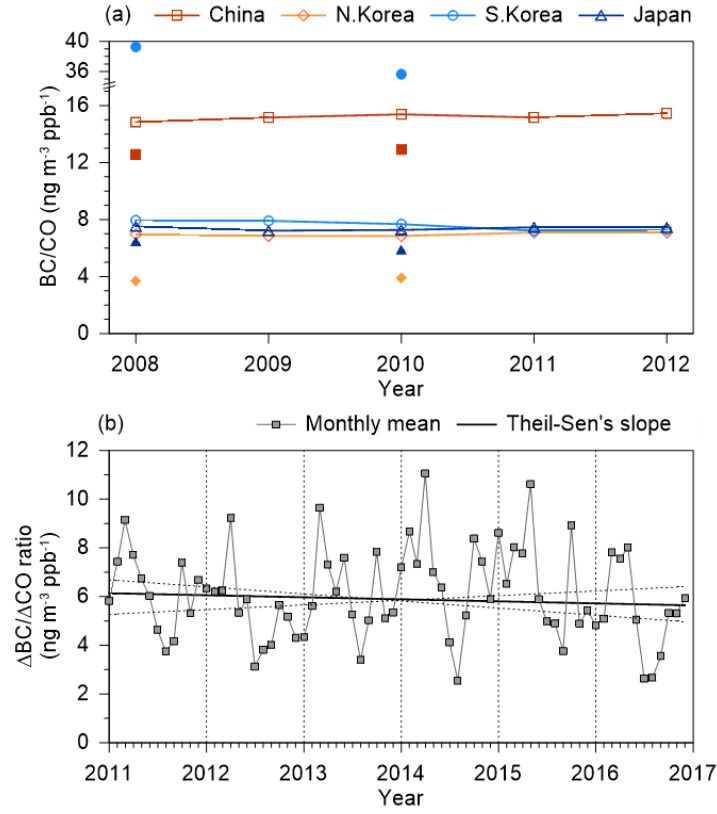

$$y = (8.21\pm0.09)\cdot\exp(-(1.32\pm1.88)\cdot10^{-3}\cdot x)$$
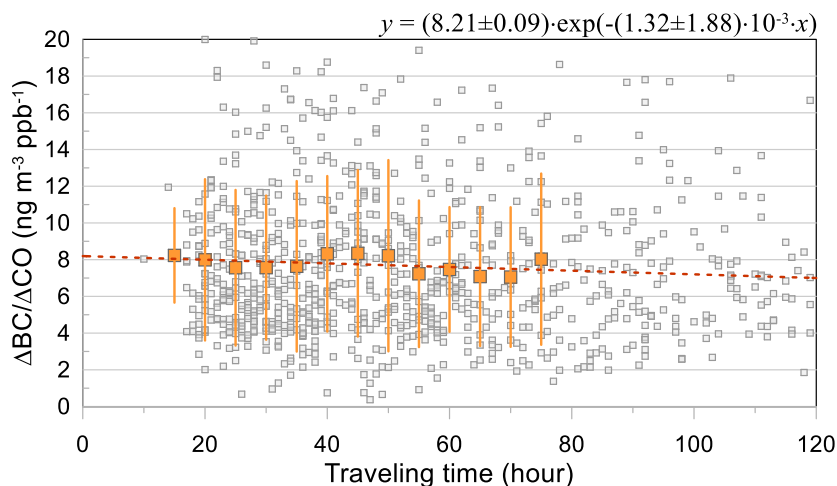
Figure S3. Scatter plot between the ΔBC/ΔCO ratio and traveling time in Noto when the APT was zero. The gray squares indicate every observed data point, and orange squares with vertical lines represent the means and standard deviations of five-hour bins for less than 72 hours. The dashed line indicates the best-fit line.
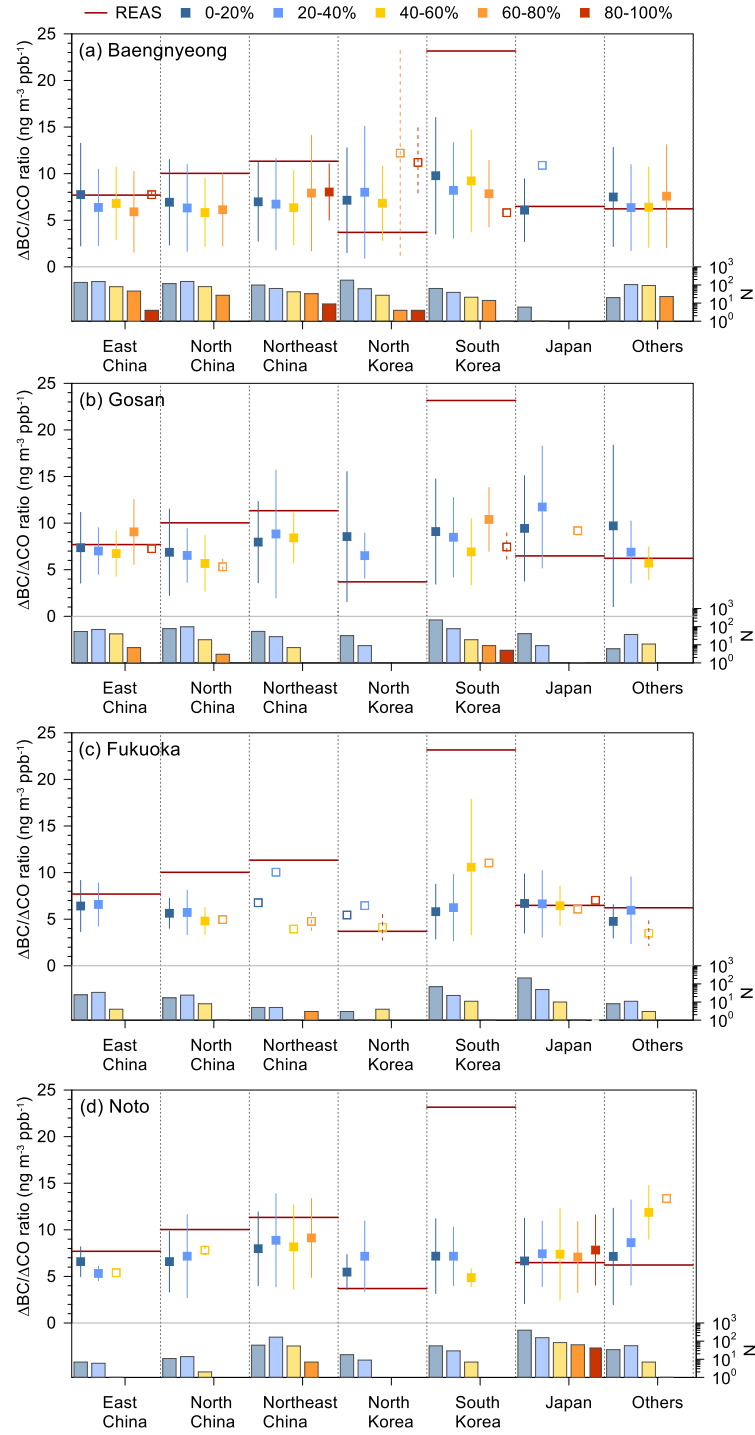
Figure S4. The measured ΔBC/ΔCO ratios at four measurement sites depending on the residence time fraction in the dominant emission region. The colored symbols with solid lines and the open symbols with dashed lines indicate the mean and standard deviation of each bin for numbers of data (N) > 5 and $N \le 5$, respectively. The bar graphs on the bottom indicate the number of data in each bin and the dominant region. The horizontal red lines depict BC/CO ratios from the REAS emission inventory.
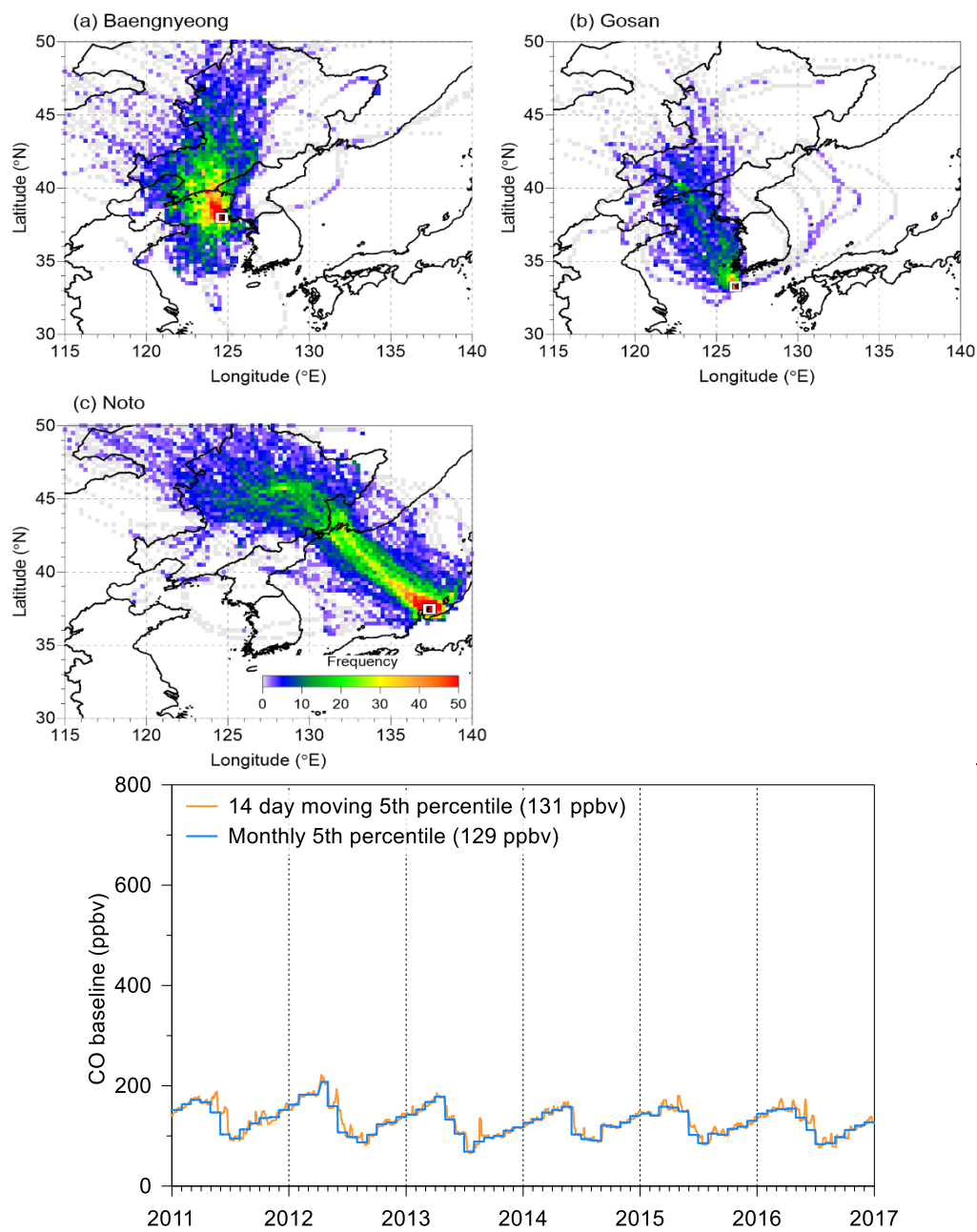
Figure S5. Time series of CO baselines calculated by different methods (14-day moving 5th and monthly 5th percentiles) at Noto.

Figure S6. (a) Time series of the BC/CO ratios from the Emissions Database for Global Atmospheric Research (EDGAR v4.3.2; open symbols) during 2008 – 2012 and MIX emission inventory (filled symbols) in 2008 and 2010. (b) Time series of the monthly means of the ΔBC/ΔCO ratio with Theil-Sen's slope during the measurement periods at Noto. The Theil-Sen's slope of the ΔBC/ΔCO ratio indicated a slight decreasing trend of the ΔBC/ΔCO ratio at -0.08/year; but the trend was statistically insignificant (*p* > 0.1). Insignificant trends of the ΔBC/ΔCO ratio were also observed at the other sites.
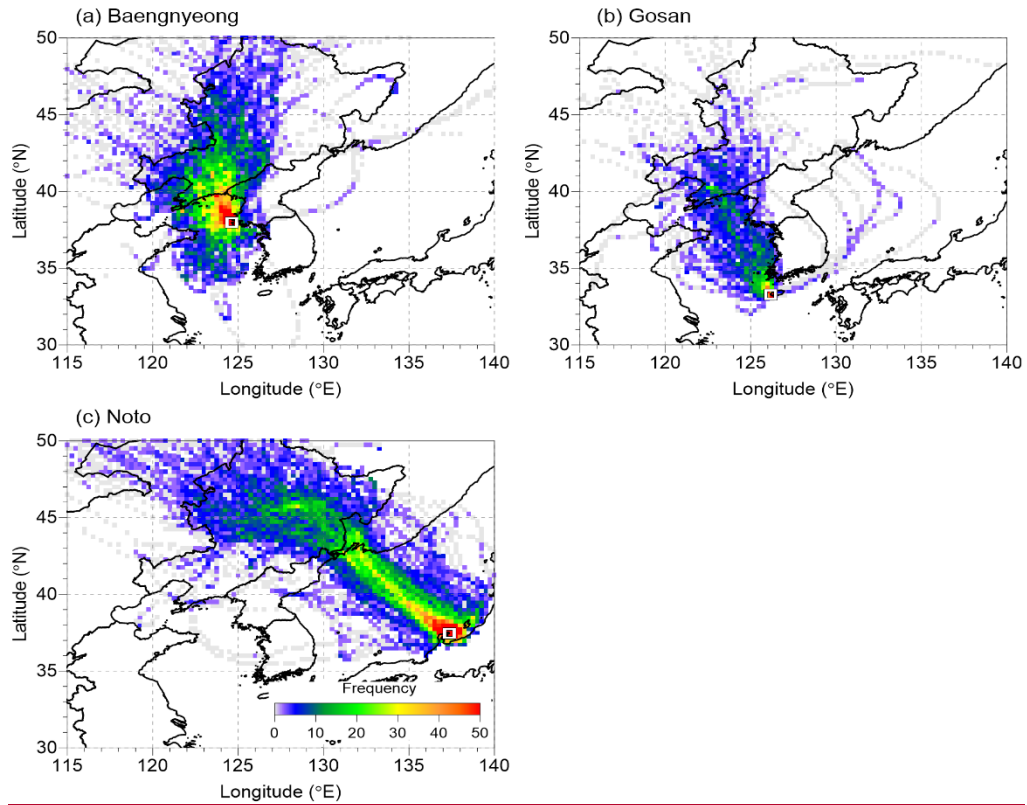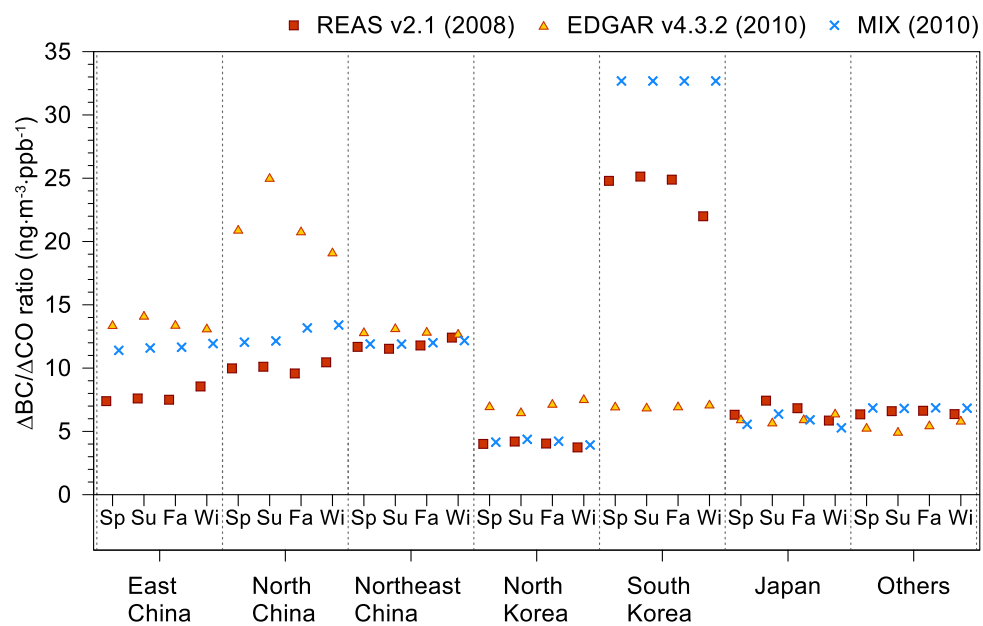
Figure S7. Same as Figure S1, except for the backward trajectory from Northeast China.
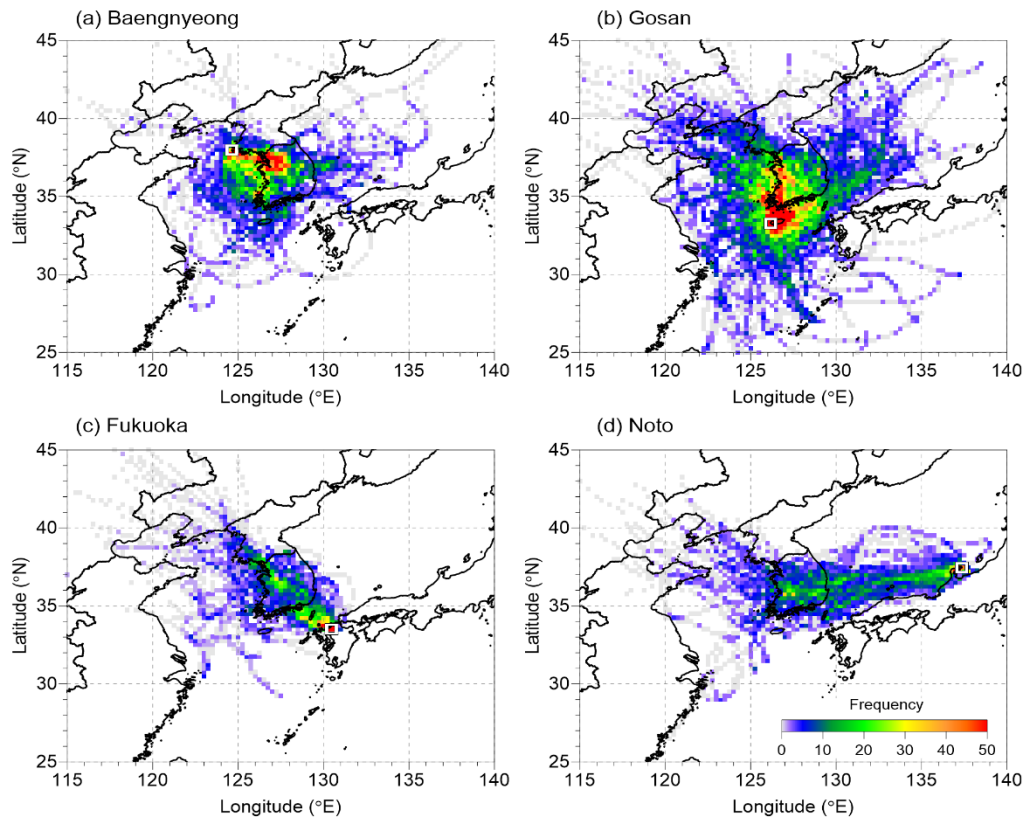
Figure ~~S6~~**S8**. Same as Figure S1, except for the backward trajectory from South Korea.

(a) Fukuoka   (b) Noto
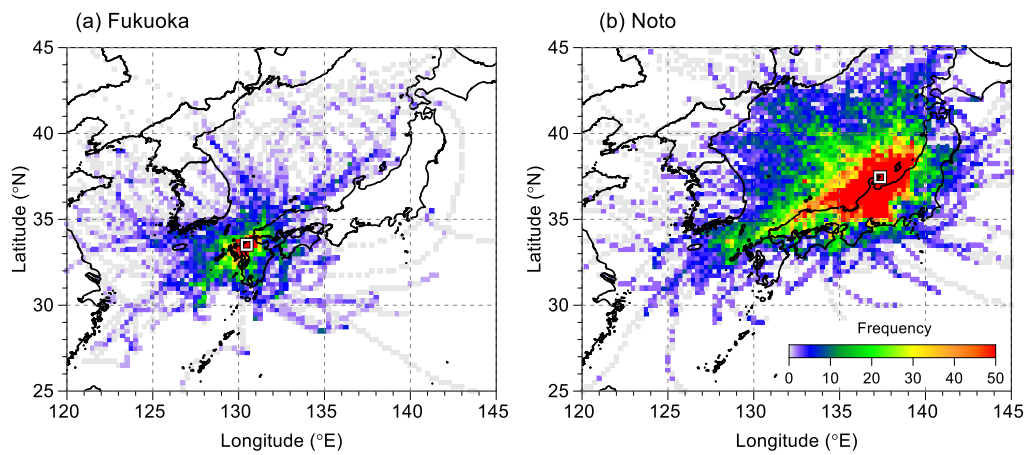
Figure ~~S7~~**S9**. Same as Figure S1, except for the backward trajectory from Japan.

Figure S10. Seasonal variations of the overall regional mean BC/CO ratio according to different bottom-up emission inventories. The number in parentheses in each inventory indicates the base year. The abbreviation of 'Sp' to 'Wi' indicates spring to winter.